Geological Analysis and Resource Assessment of selected Hydrocarbon systems

**Deliverable**

## GARAH WP2:
## 3D Pilot Study - Unconventionals

Authors and affiliation:

**Rüdiger Lutz, BGR**

**Stefan Ladage, BGR**

**Jashar Arfai, BGR**

**Susanne Nelskamp, TNO**

**Anders Mathiesen, GEUS**

**Niels Hemmingsen Schovsbo, GEUS**

E-mail of lead author:
**ruediger.lutz@bgr.de**

Version: 19.02.2021

This report is part of a project that has received funding by the European Union's Horizon 2020 research and innovation programme under grant agreement number 731166.

| Deliverable Data | | |
|---|---|---|
| **Deliverable number** | D2.4.x | |
| **Dissemination level** | Public | |
| **Deliverable name** | Resource assessment 3D pilot unconventional | |
| **Work package** | WP2., North Sea Petroleum Systems | |
| **Lead WP/Deliverable beneficiary** | GEUS/BGR | |
| **Deliverable status** | | |
| **Submitted (Author(s))** | 19/2/2021 | Rüdiger Lutz, BGR<br>Stefan Ladage, BGR<br>Jashar Arfai, BGR (now BGE[1])<br>Susanne Nelskamp, TNO<br>Anders Matthiesen, GEUS |
| **Verified (WP leader)** | 22/2/2021 | Niels Schovsbo, GEUS |
| **Approved (Coordinator)** | 24/2/2021 | Peter Britze, GEUS |

[1] BGE – Bundesgesellschaft für Endlagerung (German federal company for radioactive waste disposal)

## GENERAL INTRODUCTION

This report summarises the work carried out to assess unconventional hydrocarbon (HC) resources with a 3D basin and petroleum system model (BPSM) in a cross-border pilot study area as part of the Geo-ERA GARAH WP2: Assessment of North Sea Resources project.

In close cooperation the GARAH and 3DGEO-EU project's participants delineated the area of interest and the stratigraphic framework for the 3D basin and petroleum system modelling study. This area comprises the cross-border area of the Danish, German, and Dutch Central Graben in the central North Sea. This area has been selected based on the geological, stratigraphical and geophysical data compilation, showing reasonable cross-border coverages as well as several potential and proven petroleum source rocks.

Unconventional petroleum resources (in place) of the most important source rocks, i.e. the Jurassic Posidonia Fm, Bryne Fm and Farsund Fm, in the North Sea Central Graben were assessed for this report. The conventional resources will be assessed in a seperate report.

**TABLE OF CONTENTS**

# 1 RATIONALE AND AIMS

The overall aim of the GARAH WP2 project is to assess cross-border conventional and unconventional hydrocarbon resources in the North Sea, Europe's most prolific oil and natural gas basin. As part of this overall objective of the GARAH project, a regionally limited 3D basin and petroleum system model (BPSM) covering the Danish, German, and Dutch Central Graben area was constructed (Figure 1). This 3D BPSM model is a pilot study to reconstruct the thermal history, maturity and petroleum generation of potential and proven source rocks. As a first step we here report on modelling of the unconventional resources, meaning the shale source rocks. The conventional resources will be assessed in a separate report later as part of delivery D2.5.

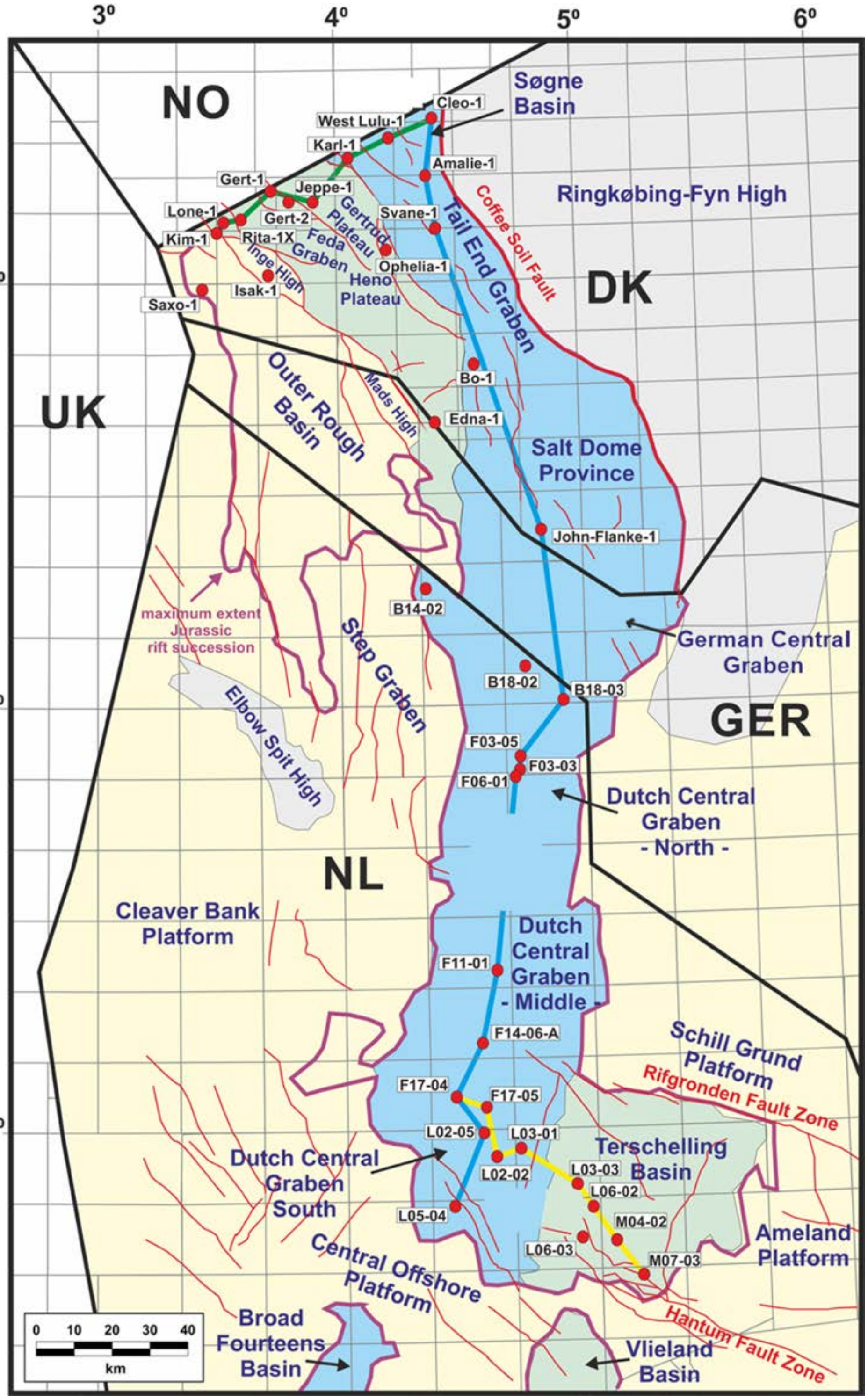


Figure 1: Geological structural elements of the study area. The Central Graben is the most prominent one, extending across the three countries (map modified from Verreussel et al., 2018)

# 2 CONSTRUCTING THE 3D PETROLEUM SYSTEM MODEL

## 2.1 Introduction

Basin and petroleum systems modelling combines seismic, geological and organic geochemical information to model the regional structural and thermal basin evolution. Based on a conceptual model which includes all available information about the geological evolution of the study area such as petrophysical and organic geochemical data, a discretised numerical model is developed. Discretisation is performed by defining vertical grid lines and horizontal event lines. For each cell, numerical input data include thickness, age at upper and lower boundary, lithological properties and heat flow. For each source rock layer, input data such as total organic carbon (TOC) content, Hydrogen Index (HI) value and a kinetic data set for petroleum generation are further required (Lutz et al., 2004). The model provides information on timing and quantities of petroleum generation and migration and it helps to focus on the parameters that affect simulation results most (Peters et al., 2012). The models are deterministic forward models, which reconstruct the burial history and all related processes, e.g. sedimentation, erosion, compaction, radiogenic heat production, petroleum generation, migration and accumulation. Details on the theoretical and numerical background are given in Hantschel and Kauerauf (2009).

The 3D BPSM pilot study utilizes structural and stratigraphic subsurface models, which are continuously developed and improved within GeoERA 3DGEO-EU project. Relevant parameter layers for petroleum system modelling and source rock formations in the pilot study area, have been compiled and provided by the project partners. During construction of the 3D BPSM these layers have been combined, aggregated and incorporated. A subset of these layers has been provided to the Information Platform of GeoERA.

## 2.2 Area of Interest

In close cooperation the GARAH and 3DGEO-EU project's participants delineated the area of interest and the stratigraphic framework (Thöle et al., 2019) for the 3D basin and petroleum system modelling study (Figure 2). This area comprises the cross-border area of the Danish, German, and Dutch Central Graben in the central North Sea. This area has been selected based on the geological, stratigraphical and geophysical data compilation, showing reasonable cross-border coverages as well as several potential petroleum source rocks.

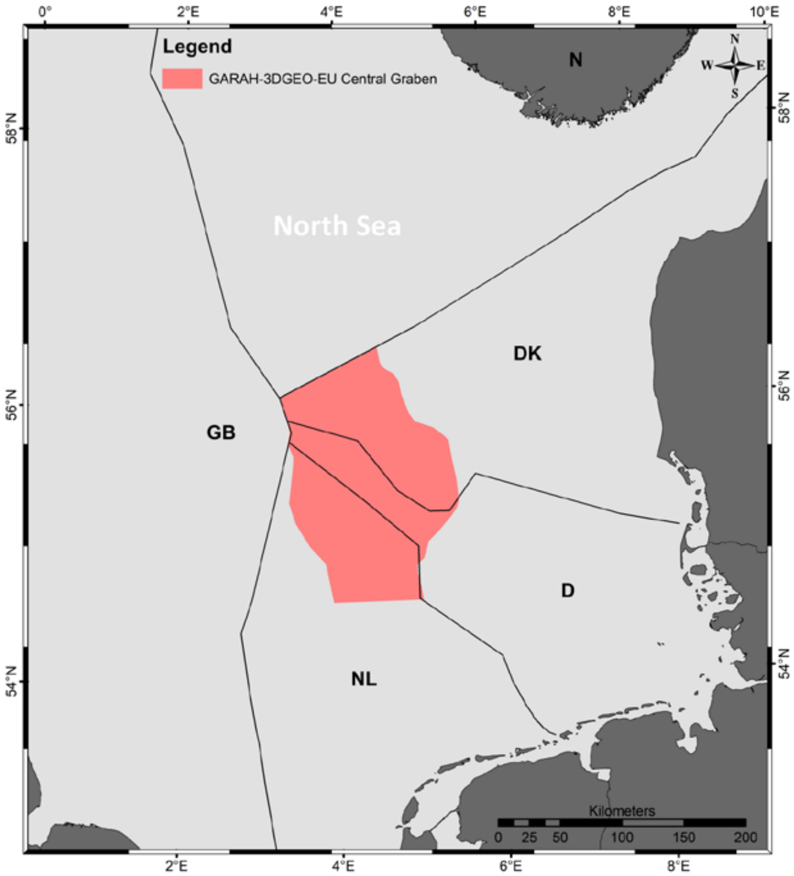


**Figure 2** Location map of the central North Sea with outlines of the maritime borders. The 3D pilot study area is shown in red. It comprises the “Entenschnabel” in the German sector and adjacent Dutch and Danish offshore areas.

## 2.3 Stratigraphic Framework

Nine key horizons have been selected for building the stratigraphic framework of the 3D basin model in the central North Sea (Figure 3). These are:

0. Sea floor
1. MMU – Mid-Miocene Unconformity
2. Near base Tertiary
3. Base Upper Cretaceous
4. Near base Lower Cretaceous
5. Posidonia Shale / Toarcian
6. Near Base Lower Jurassic
7. Near base Middle Triassic
8. Top Zechstein
9. Base Zechstein

For building the key horizon grids a workflow has been agreed upon by the project partners. Each horizon and its corresponding grid or point data in time domain, whichever is available, is merged to a time grid covering the pilot study area. These are cross-checked and corrected for obvious geological inconsistencies (e.g. such as cross-cutting layers). These time grids are then depth converted using the TNO procedure and algorithms for depth conversion (Doornenbal et al., 2019; Pluymaekers et al. 2017). Resolution of the grids is 250 m x 250 m and coordinates are given in UTM 31 N (WGS 84).

One of the 3DGEO-EU project objectives is to reduce discrepancies and enhance the quality of cross-border geological features and interpretations in the central North Sea. Highest quality horizon grids are thus expected to be delivered at the end of the 3DGEO-EU project. The 3D pilot study therefore started by incorporating merged horizon grids, even though significant cross-border issues might still exist. Thus, the first task was to identify the cross-border issues and develop workflows to eliminate them. The 3D model of this work package can later be updated as higher quality horizon grids are prepared by the 3DGEO-EU project. A comprehensive report on the current state of the art on cross-border issues is given in the QC report of the 3DGEO-EU project (Thöle et al., 2019).

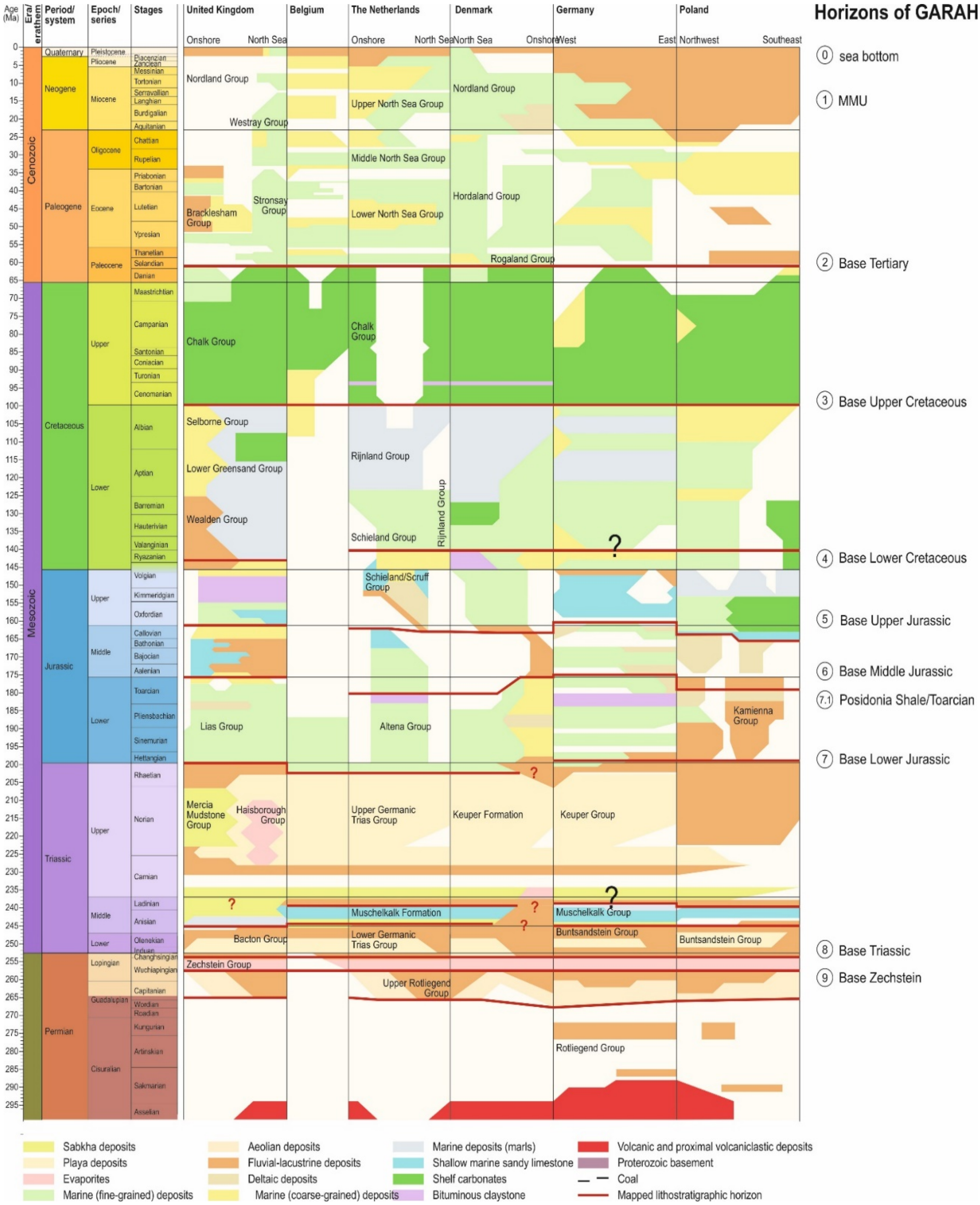


Figure 3: Stratigraphic framework after Doornenbal and Stevenson (2010) and key horizons annotated to the right, which were used for construction of the 3D basin model.

## 2.4 Methods and data base

3D petroleum system modelling was carried out with the software PetroMod 2019.1.

A set of attributes and parameters have been defined, which are necessary for building the model:

1. Present-day input
   - Absolute ages of horizons
   - Lithology
   - Facies maps

2. Paleo Geometry
   - Erosion events
   - Erosion maps - Paleo thicknesses of eroded formations
   - Salt maps, initial salt thicknesses, salt activity during basin evolution

3. Boundary conditions
   - Sediment Water Interface Temperature (SWIT)
   - Heat flow data
   - Paleo water depths

4. Calibration data
   - Vitrinite reflectance data
   - $T_{max}$
   - Temperature

5. Source rocks and their properties
   - Upper Jurassic (Farsund Fm, Bo Member)
   - Middle Jurassic (Bryne Fm)
   - Lower Jurassic (Posidonia Shale Fm)

6. Reservoir rocks

The input parameters, which are necessary to build the 3D model are shown in Appendix 1.

For the calculation of vitrinite reflectance from temperature histories, the EASY%Ro algorithm of Sweeney & Burnham (1990) is used. This calculation method follows a kinetic reaction scheme and is valid for calculated reflectance values between 0.3 and 4.5 % vitrinite reflectance (VR).

### 2.4.1 *Time – Depth Conversion*

The present-day stratigraphic and structural framework of the model from the base Zechstein to Present is provided by using structural depth maps with a resolution of 250 x 250 m cell size. Depth conversion was done using a velocity model. The purpose of this velocity model is the time depth conversion of the seismic interpreted time-grids to depth (Doornenbal et al., 2019).

Well information from 63 wells covering the study area were available and 48 of the wells had vitrinite data available for calibration (Figure 4).

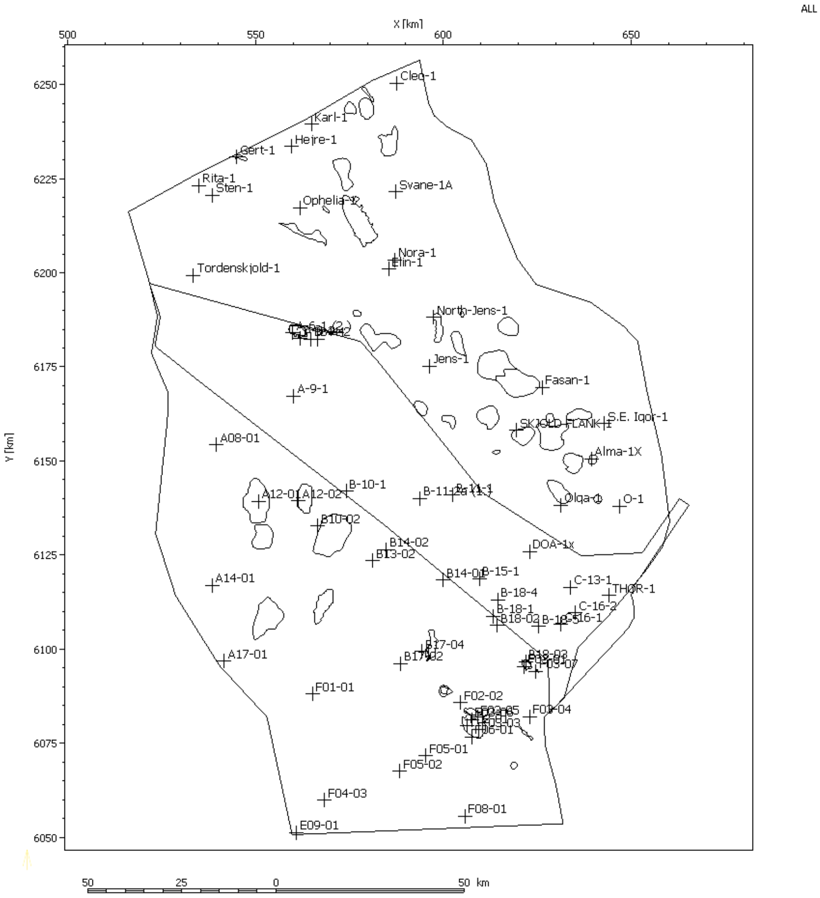


Figure 4: Location of wells integrated into the 3D BPSM. Crosses show well locations, small polygons indicate oil or gas fields, large outer polygon outlines the study area. The large polygon in the middle is the German Entenschnabel area.

## 2.5 Geological Model

The input model consists of ten layers covering a time interval from the Zechstein to the present. A sedimentary basement of 2000 m thickness for the pre-

Zechstein formations was added to extend the 3D model below the Upper Permian.

In this study, an initial thickness of 700 m is assumed for the Zechstein layer (Ten Veen et al. 2012) before halokinesis ultimately formed salt diapirs (Figure 5).

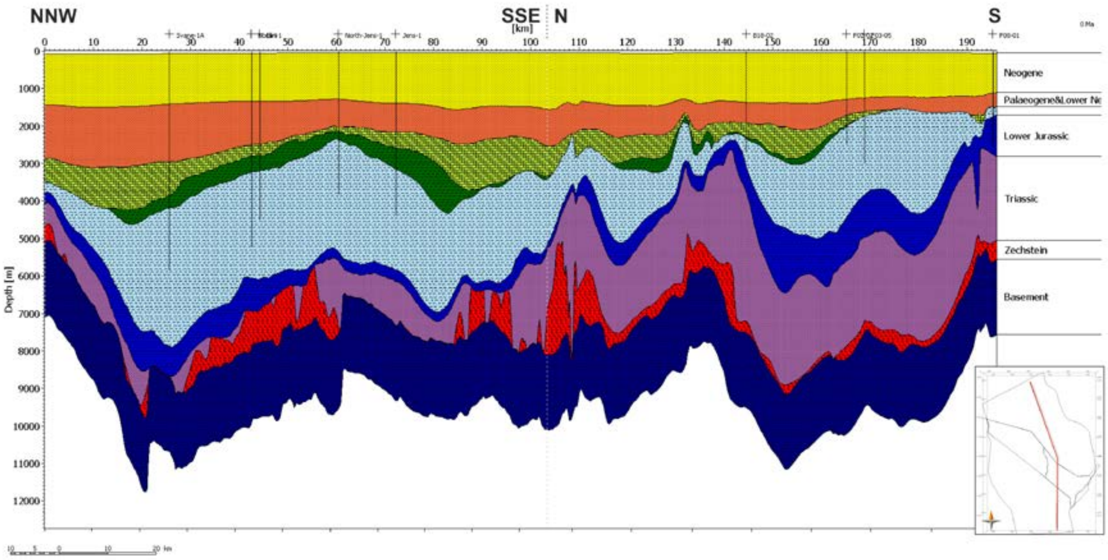


Figure 5: 2D cross section across the 3D model showing the sedimentary layers and the salt diapirs (red). Red line in inset map shows profile line.

Four erosional phases are included in the basin model: the Mid-Cimmerian (Mid-Jurassic), the Late Cimmerian (Early Cretaceous), the Subhercynian inversion (Late Cretaceous), and a final one during Mid Miocene time (Figure 6).

The domal uplift during the Mid-Cimmmerian phase resulted in a widespread erosion in large parts of the study area. The intensity and amount of erosion varied in the area, depending on the structural elements (basin, high, platform). The erosion event began during the Bathonian (165 Ma) and ended in the Oxfordian (158 Ma). Layers that were affected by this erosional phase include Triassic and Lower to Middle Jurassic sediments. The Late Cimmerian erosion phase (from 122 Ma to 98.9 Ma) affected the Dutch and Danish North Sea area and partly eroded Upper Jurassic sediments.

| | Age [Ma] | Horizon | - | Depth Map | Layer |
|---|---|---|---|---|---|
| 1 | 0.00 | Horizon_0 | | Seafloor | Neogene |
| 2 | 11.20 | MMU | | | Erosion_17 |
| 3 | 15.97 | Horizon_1 | | MMU_DE_NL_DK | Palaeogene&Lower Neogene |
| 4 | 61.60 | Horizon_2 | | Base_Tertiary_DE_NL_DK | Upper Cretaceous |
| 5 | 83.50 | Sub-Hercynian | | | Erosion_65 |
| 6 | 98.90 | Horizon_3 | | Upper_Cretaceous_DE_NL_DK | Lower Cretaceous |
| 7 | 122.00 | Late-Cimmerian | | Late-Cimmerian | Late-Cimmerian |
| 8 | 142.00 | Horizon_4 | | Base_Cretaceous_DE_NL_DK | Upper Jurassic |
| 9 | 158.00 | Mid-Cimmerian | | | Erosion_32 |
| 10 | 165.50 | Horizon_5 | | Upper_Jurassic_DE_NL_DK | Lower Jurassic |
| 11 | 201.30 | Horizon_6 | | Base_Jurassic_DE_NL_DK | Triassic |
| 12 | 251.00 | Horizon_7 | | Base_Lower_Triassic_no_diapir | Zechstein |
| 13 | 258.00 | Horizon_8 | | Base_Zechstein_DE_NL_DK | Basement |
| 14 | 380.00 | Horizon_18 | | Basement | |

Figure 6: Stratigraphic succession of the 3D model and assigned ages to the individual sedimentation and erosion events. Light green rows indicate erosion. The Late Cimmerian event is characterized by deposition in Germany and erosion in Denmark and the Netherlands.

A major Late Cretaceous inversion phase in the North Sea basin resulted in uplift and erosion of the sedimentary fill in different pulses and is called the Subhercynian erosional event. Partly, Upper Jurassic, Lower Cretaceous and Upper Cretaceous sediments were eroded in the central and northwestern part of the study area. Here, erosion during the Late Cretaceous was active in our model between 98.9–83.5 Ma. The final erosion during the Mid-Miocene with a duration of ~5 Ma (from 15.97 Ma to 11.2 Ma) is included with an erosion thickness of 30 m (Figure 6). Assigned lithology for each of the layers is based on generalised well descriptions within the study area.

Paleo thickness values are estimated and based on Arfai and Lutz (2017) and seismic interpretation results covering basin and graben formations for the German North Sea. Eroded thicknesses for Denmark and the Netherlands were provided by GEUS and TNO, respectively.

The two most important source rocks of the North Sea are the Upper Jurassic Bo Member of the Farsund Fm and the Lower Jurassic Posidonia Shale Fm. The Bo

Member is the main source rock for the oil fields in Denmark and likely extends partly into Germany. The Posidonia Shale Fm is an important oil source rock in the Netherlands and also extends into Germany. The Bryne Fm includes coals in the Middle Jurassic in Denmark only.

The Posidonia Shale source rock is characterised in our model with an average TOC content of 5 wt% in Germany and a TOC map for the Netherlands with values ranging between 3.55 and 4.96 wt%, and an HI value of 500 mg HC/g TOC. The Farsund Fm (Bo Mb) source rock is defined with a TOC content of 5 wt% and an HI value of 400 mg HC/g TOC. The Bryne Fm has a TOC content of 70 wt% and an HI value of 300 mg HC/g TOC.

Hydrocarbon generation of the Posidonia Shale Fm and Farsund Fm was calculated using the kinetic data set of Pepper & Corvi (1995) type TII(B) and the Bryne Fm was assigned the reaction kinetic Pepper & Corvi (1995) type TIIIH(DE). A 3D view of the model is shown in Figure 7.

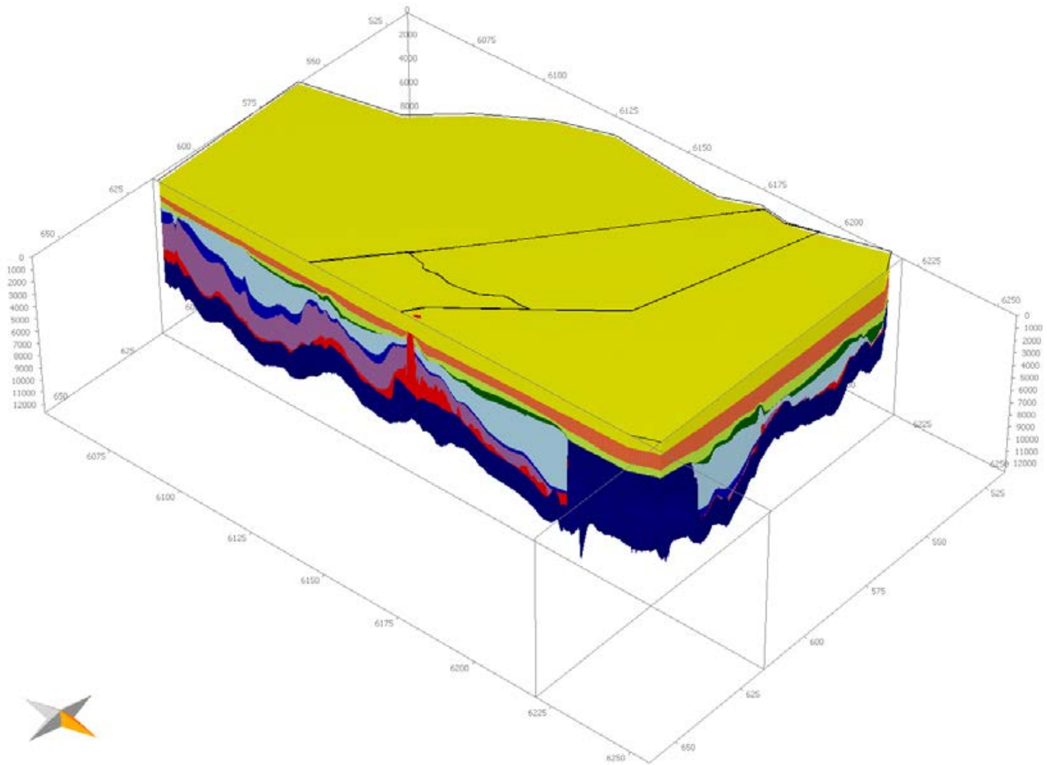

Figure 7: View from the NE into the 3D model. The Eastern and northern sides are cut off for a better view into the model. Red layer is Zechstein salt and light blue layer is Upper-Middle Jurassic.

## 2.6 Boundary conditions

### *2.6.1 Palaeo Water Depth (PWD)*

The paleo water depths *(*PWD) curve used in the model was constructed based on PWD trends of adjacent areas in the southern Dutch Central Graben (Verweij et al. 2009; Abdul Fattah et al. 2012a, b; Arfai & Lutz 2017). The paleo water depths were allowed to vary in time but were kept constant over the entire area at a certain time. The PWD is less than 100 m with shallowing during erosion phases and deepening in-between.

### *2.6.2 Sediment Water Interface Temperature (SWIT)*

The paleo surface temperature at the sediment water interface was calculated with an integrated software tool that takes into account the paleo water depth and the paleo latitude of the study area (Wygrala 1989).

### *2.6.3 Basal Heat Flow*

The main heat flow trend is based on the McKenzie model for a passive margin (North Sea basin), and is also adopted from studies covering the adjacent areas (Verweij et al. 2009; Abdul Fattah et al. 2012a, b; Arfai & Lutz 2017). One heat flow trend was assigned to the Step Graben System and a different one to the Central Graben.

During the Early Triassic (251 Ma) a peak (63 mW/m²) is included in the heat flow trend attributed to first post-orogenic (Variscan orogeny) rifting phases. This rifting stage is characterised by the beginning of graben formation and subsequent Triassic–Middle Jurassic tectonic subsidence and thickening of sediments within the Central Graben area. A second increase (85 mW/m²) during the Late Jurassic at 158 Ma represents the main heat flow event in the Central Graben area (Figure 8). This major extensional phase during the Late Jurassic formed the present-day Central Graben geometry. Subsequent Cretaceous and Cenozoic subsidence was largely controlled by a phase of post-rift thermal subsidence. The compressional stress regime resulted in several phases of basin inversion during the Late Cretaceous. However, this event had only a minor impact on the heat flow history and we assigned a heat flow value of 65 mW/m² for this time period. The present-day heat flow was calibrated based on temperature and vitrinite reflectance data.

The heat flow trend for the Step Graben System is the same as for the Central Graben until the Mid-Jurassic. The Late Jurassic rifting of the Central Graben is omitted in the Step Graben heat flow trend (Figure 8). The values decrease constantly from the Mid-Jurassic to the present-day value of 52 mW/m².

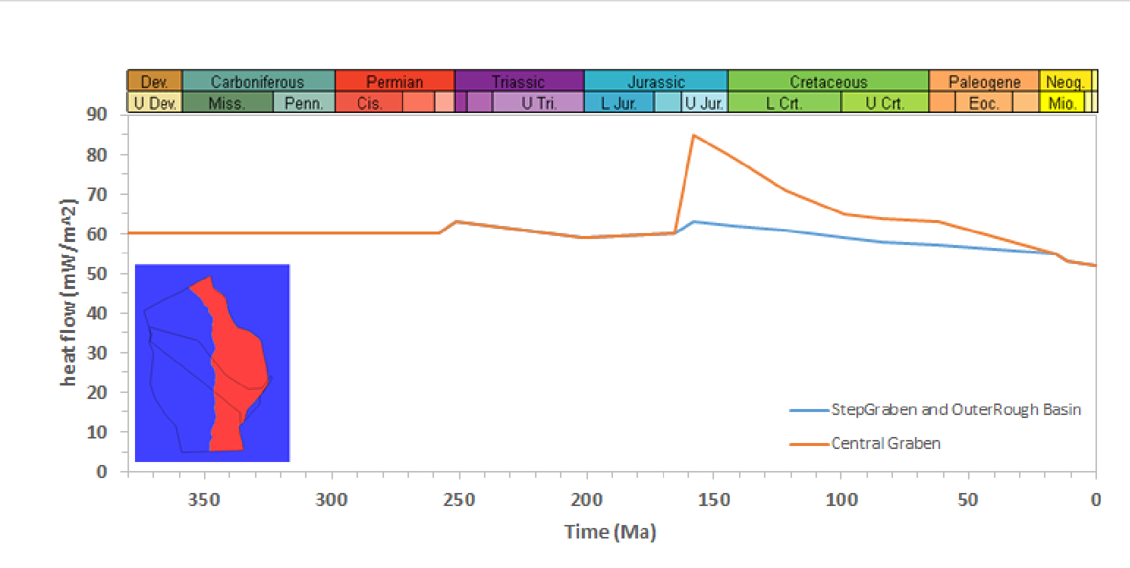


Figure 8: Heat flow trends for the pilot study area. Blue is the heat flow trend assigned to the area outside the Central Graben and red is the heat flow trend within the Central Graben. Inset shows the heat flow trend assignment in map view.

An alternative heat flow model was also calculated to test the influence of different heat flow scenarios on the simulation results. This tectonic heat flow model uses a multi 1D approach and takes into account transient effects of sediment infill and erosion using the inversion of subsidence curves to model changes in crustal heat production over time and space (Van Wees et al., 2009, Bonté et al., 2020). The same depth and thickness maps, water depth, sediment surface temperature, as well as erosion maps were used as input data for the model. In addition a standard model for the crustal and lithosphere thickness and thermal properties was used (Bonté et al., 2020) and an uncertainty range was assigned to these properties. The tectonic history of the area is defined by assigning different streching models using the crustal and lithospheric stretching factors δ and β, respectively. The model then calculates the tectonic subsidence for the each of the multi 1D pseudo wells and compares the modelled tectonic subsidence to the observed. Based on this tectonic model, the input parameter, and their uncertainties a Monte Carlo calculation is performed to calculate the basal heat flow distribution for each pseudo 1D point in the area through time. The main result of the model can be expressed as mean, minimum, maximum as well as P10, P50 and P90 distributions. The input heat flow maps used are the P50 result of the heat flow model and are shown in Appendix 2.

Generally a slightly better fit between measured and calculated vitrinite reflectance values was achieved with the default heat flow model (Figure 9). The main difference between the models is the timing of maximum temperature. While the default model assumed a heat flow peak in the Central Graben area during the Jurassic, the alternative model assumes highest temperatures during the Cenozoic. All calibration plots are shown in Appendix 3.

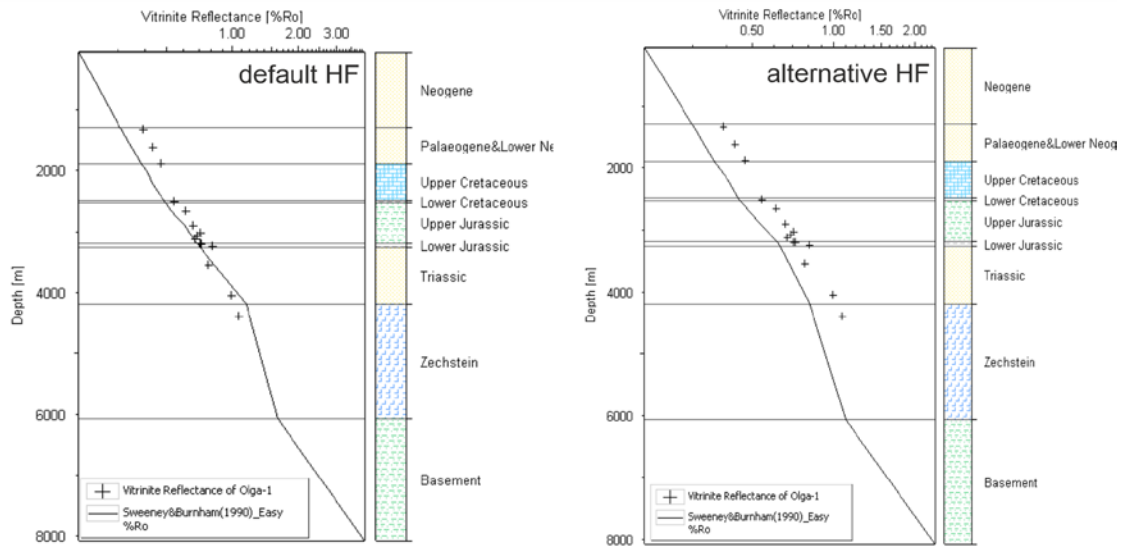


Figure 9: Calculated (solid line) and measured vitrinite reflectance for one well in the Danish Central Graben. Left are the results for the model with the default (McKenzie) heat flow and right are the results for the alternative heat flow model. A better fit was achieved with the default heat flow.

## 3 3D BPSM SIMULATIONS

For unconventional petroleum systems, we are interested in the hydrocarbons generated that have not yet been expelled. In this system, oil or gas remains in the source rock (i.e. source rock = reservoir) thus the amount of hydrocarbons retained in the source rock are important. These hydrocarbons are either

adsorbed or retained as free gas in the source rock. The saturation end point for oil (critical oil saturation) controls expulsion, because it defines a threshold saturation which has to be overcome before oil starts to move and is expelled. In this study we used a critical oil saturation ($S_{oc}$) of 3 % and a critical gas saturation ($S_{gc}$) of 0 %. These two values are important for the free oil and gas phases. Expulsion is additionally controlled by the capillary pressure difference between the source rock and the surrounding rocks.
Hydrocarbons are adsorbed on kerogen (Ker). Therefore, the amount of adsorbed oil and gas is controlled in the simulations by the amount of kerogen available for adsorption. The sorption ratios are defined as 0.02 g/gKerC for gas and 0.1 g/gKerC for oil, respectively.

In contrast to probabilistic simulations, where 10,000-100,000 calculations can be easily realized, the number of possible simulation runs for full 3D models are limited due to the long simulation times. Simulation times for our models varied between 5 h and 42 h. Nevertheless, the impact of the most important parameters on the results can be assessed by simulating scenarios with varying values for these parameters. We calculated several models, where the following parameters were varied systematically,

- heat flow evolution
- lithology around source rock
- critical oil saturation
- sorption ratio of oil on kerogen.

The structural model was built with the input parameters as described above and constitutes the starting model (Figure 10). The parameter tests were performed on the full 3D model containing all source rocks. In order to save computation time for the parameter tests we sampled the models in x-y direction two-fold and reduced the number of sublayers in the Lower Jurassic to Upper Cretaceous layers. This step reduced the total amount of retained petroleum by only 3 %.
We employed the McKenzie heat flow model to derive the default heat flow evolution in the study area. Using the alternative heat flow model (see section

2.6.3) in the simulation results in about 9 % less petroleum (oil+gas) accumulated in the source rocks. Changing the lithology around the source rocks from siltstones to sandstones allows more expulsion of petroleum out of the source rock and reduces the accumulated amount of petroleum in the source rock by around 17 % (Figure 10).

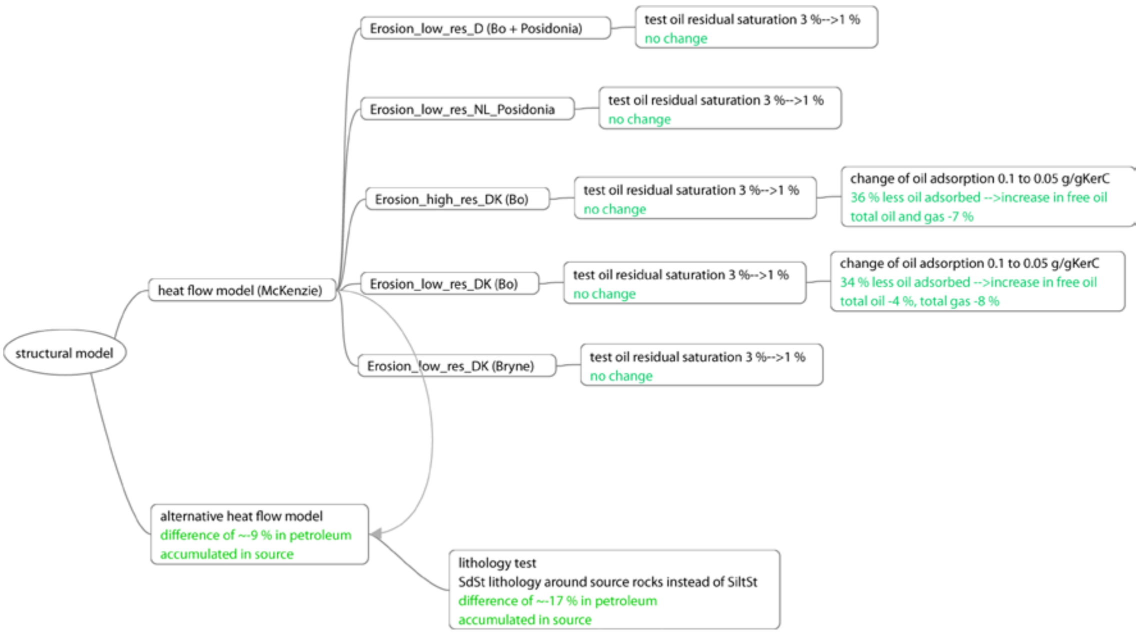


Figure 10: Workflow scheme to illustrate the different models used to assess the effects of the key parameters on the simulation results.

We conducted the parameter test on critical oil saturation with different models for each source rock in the three countries. These tests showed that critical oil saturation had no effect on the amount of retained petroleum in all of the reduced resolution models, i.e. models with a reduced number of sublayers (z direction) (Figure 10). The parameter oil adsorption was tested on the Danish source rock Bo Mb of the Farsund Fm. Here, we reduced the sorption capacity of oil from 0.1 g/gKerC to 0.05 g/gKerC. This resulted in 34 % less adsorbed oil but increased the amount of free oil in the pore space. Thus the total amount of retained oil is only 4 % less. To a certain extent this comes at the expense of retained gas, which decreases by around 8 %.

The influence of these parameters “critical oil saturation” and “oil sorption” were additionally studied with the full resolution model for the Bo Mb source rock.

Decreasing the “critical oil saturation” of the Bo Mb source rock in the full resolution model again had no effect on the amount of retained petroleum. The reduction of the oil sorption capacity in the full resolution model had the same effect as in the low resolution model. The adsorbed oil amount was reduced by 36 %, free oil increased and total retained oil and gas amounts decreased by around 7 % (Table 1).

Table 1: Calculated free, adsorbed and total amounts of oil and gas for the various parameter test models

| | 3D BPSM model GARAH | | | | | | | |
|---|---|---|---|---|---|---|---|---|
| | GIIP | | | OIIP | | | ical oil saturat | Oil sorption |
| | free | adsorbed | total | free | adsorbed | total | Soc | |
| Model | | (10^9 m^3) | | | (10^6 t) | | (%) | (g/gKerC) |
| Erosion_low_res_D (Posidonia) | 10.2 | 11.4 | 21.7 | 100.7 | 133.3 | 234.0 | 3 | 0.1 |
| Erosion_low_res_D (Bo) | 0.5 | 1.5 | 2.0 | 6.3 | 62.0 | 68.3 | 3 | 0.1 |
| Erosion_low_res_NL_Posidonia | 24.3 | 13.1 | 37.4 | 102.1 | 47.7 | 149.8 | 3 | 0.1 |
| Erosion_low_res_DK_Bo | 6.9 | 137.0 | 143.9 | 1023.0 | 2671.6 | 3694.6 | 3 | 0.1 |
| Erosion_low_res_DK_Bryne | 131.1 | 4115.5 | 4246.6 | 0.0 | 3022.6 | 3022.6 | 3 | 0.1 |
| Erosion_low_res_D (Posidonia) | 10.2 | 11.4 | 21.7 | 100.7 | 133.3 | 234.0 | 1 | 0.1 |
| Erosion_low_res_D (Bo) | 0.5 | 1.5 | 2.0 | 6.3 | 62.03 | 68.3 | 1 | 0.1 |
| Erosion_low_res_NL_Posidonia | 24.3 | 13.1 | 37.4 | 102.1 | 47.7 | 149.8 | 1 | 0.1 |
| Erosion_low_res_DK_Bryne | 131.1 | 4115.5 | 4246.6 | 0.0 | 3022.6 | 3022.6 | 1 | 0.1 |
| Erosion_low_res_DK_Bo | 6.9 | 137.0 | 143.9 | 1023.0 | 2671.7 | 3694.7 | 1 | 0.1 |
| Erosion_low_res_DK_Bo | 4.0 | 128.3 | 132.3 | 1784.9 | 1760.8 | 3545.7 | 1 | 0.05 |
| Erosion_high_res_DK_Bo | 7.9 | 157.2 | 165.1 | 2082.8 | 2020.7 | 4103.5 | 1 | 0.05 |
| Erosion_high_res_DK_Bo | 10.0 | 168.2 | 178.2 | 1247.3 | 3147.0 | 4394.3 | 1 | 0.1 |
| Erosion_high_res_DK_Bo | 10.0 | 168.2 | 178.2 | 1247.3 | 3147.0 | 4394.3 | 3 | 0.1 |

# 4 RESULTS

## 4.1 Final 3D BPSM

The model presented here is the first public 3D basin and petroleum system combined model across the Danish, German and Dutch Central Graben area. The vitrinite reflectance overlay on the Upper and Lower Jurassic (Figure 11 and Figure 12) layer shows the complex varying cross-border present day thermal maturity distribution. This maturity distribution highlights the different structural settings and basin evolution across and on both sides of this part of the Central Graben, with the German part acting as a structural high. The Upper Jurassic (Figure 11) is in the oil window for the largest part of the Danish portion of the study area. In contrast, in the German part of the study area in general only the early oil window is reached and only in few, fragmented, small patches, especially outside the Central Graben area sensu stricto, in the Outer Rough Basin (see also Figure 1 for structural elements). In the Dutch North Sea the Upper Jurassic is also only marginally mature, i.e. partially in the early oil window.

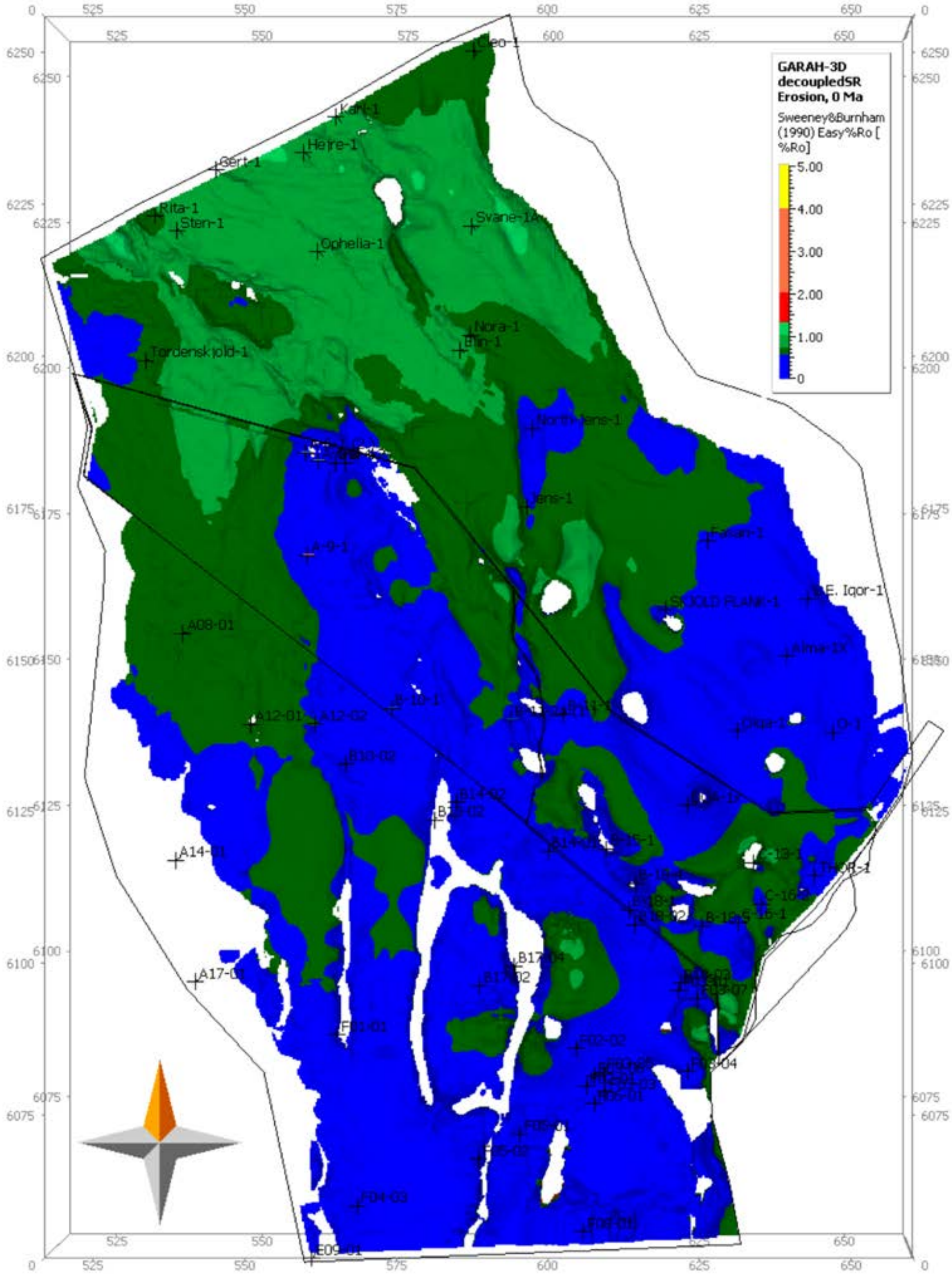


Figure 11: Calculated vitrinite reflectance at the top of the Mesozoic pre-Cretaceous sediments, i.e. mostly top Upper Jurassic, where missing top Lower Jurassic or Triassic. Blue=immature, green=oil window.

The maturity of the Lower Jurassic is significantly higher than that of the Upper Jurassic. Highest maturities are again reached in the Danish North Sea, where large parts are in the gas window or are already overmature. Toward the south and into the German North Sea, maturity decreases and oil window maturities are reached. Into the Dutch North Sea, maturities increase and the gas window is reached.

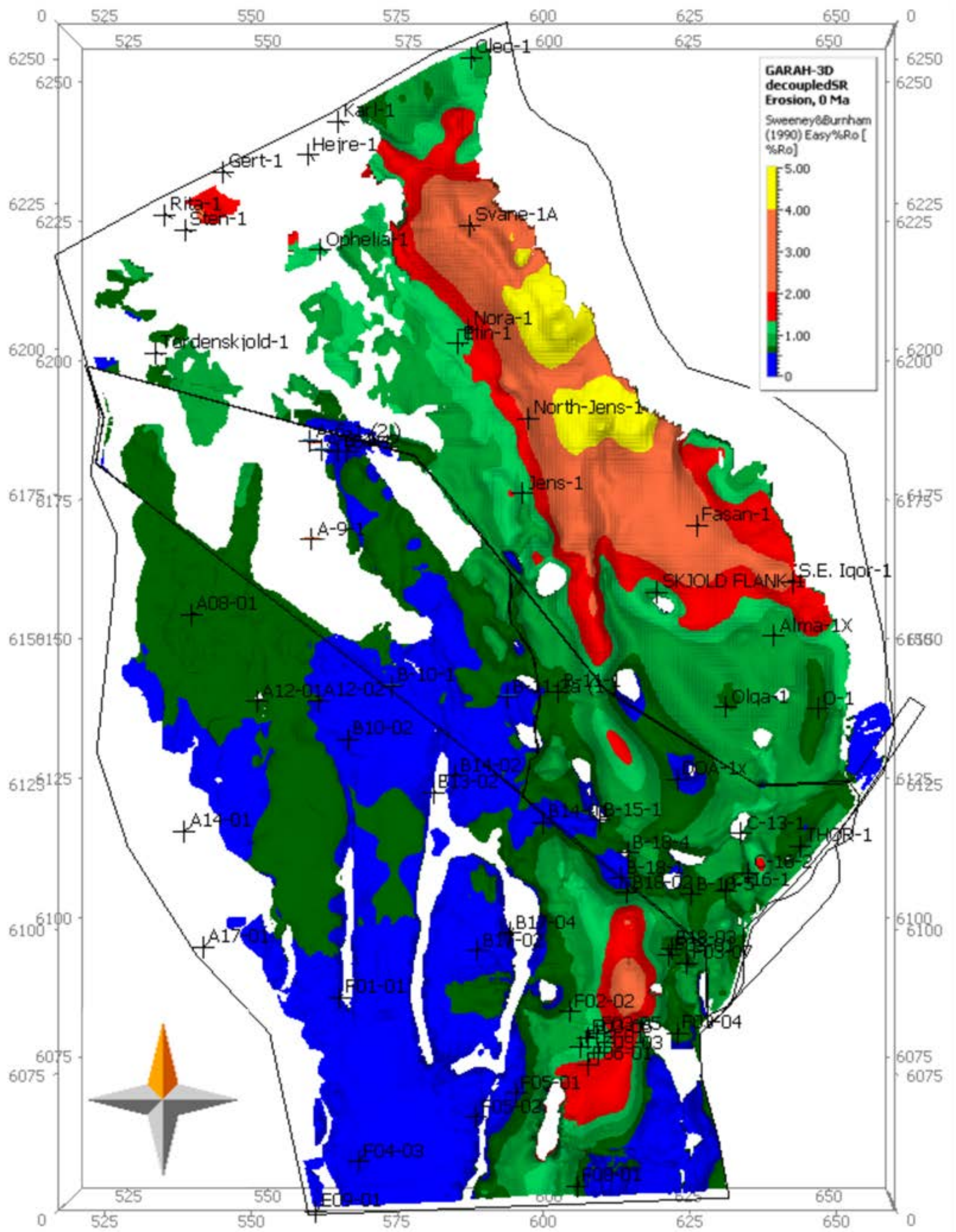


Figure 12: Calculated vitrinite reflectance at the top of the Mesozoic pre-Upper Jurassic sediments, i.e. mostly top Lower Jurassic, where missing top Triassic. Blue=immature, green=oil window, red=gas window, yellow=overmature.

The different source rock maturity resulted in different amounts of generated petroleum across the 3D model (Figure 13). The transformation ratio of the Bo Mb source rock in Denmark is shown in Figure 14 and also highlights the different maturities in the Danish North Sea.

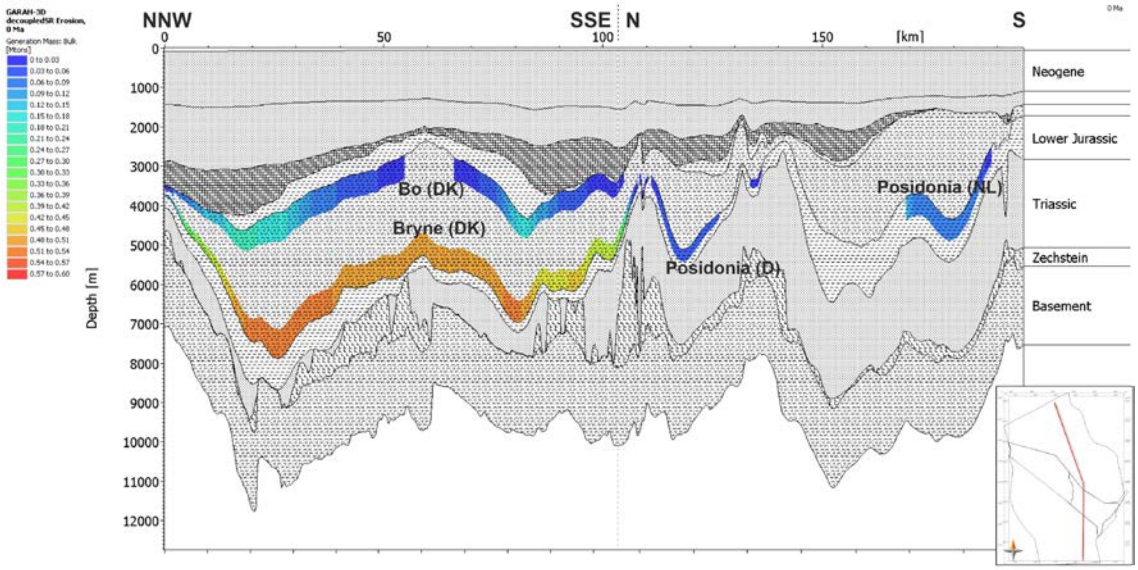


Figure 13: 2D cross section across the 3D model showing the generated mass of petroleum for the source rocks. Red line in inset map shows profile line and it is the same as in Figure 5. NB: The Upper Jurassic Bo Mb. source rock in Germany did not generate petroleum, because of insufficient maturity. The values are shown for each cell and do not represent the true source rock thickness.

The final results were calculated with the high resolution models, using a residual oil saturation of 3 % and an oil sorption of 0.1 g/gKerC. A gas density of 0.85 kg/m$^3$ was used to convert from mass to volume of gas. Specified are the accumulated amounts in the source rock. i.e. oil and gas in-place. However, technically recoverable resources - not determined in this study - will be significantly less, in general at least one order of magnitude.

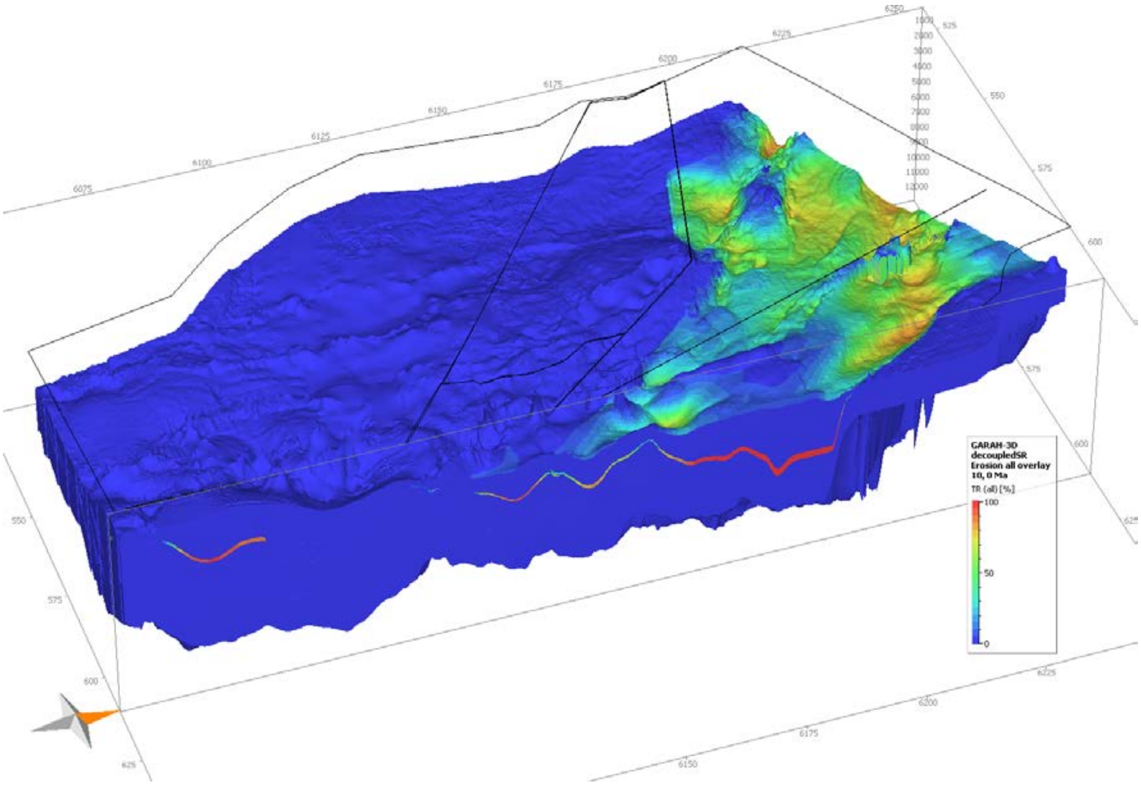


Figure 14: Transformation ratio at the top of the Upper Jurassic layer. Colored line at the side are deeper lying source rocks.

## 4.2 In-place resources

### *4.2.1 Denmark*

The Bo source rock in the 3D model accumulated around $178 \times 10^9$ $m^3$ of natural gas and around $4{,}400 \times 10^6$ t of oil. The amounts of adsorbed oil and gas are larger than the respective amounts of their free phase (Table 2).

The Bryne source rock with its more humic type of organic matter accumulated around $4200 \times 10^9$ $m^3$ of natural gas and around $2{,}900 \times 10^6$ t of oil. The deeper burial of the source rock compared to the Bo source rock results in a higher share of adsorbed gas than free gas and the oil is completely adsorbed.

Both source rocks together accumulated $4{,}400 \times 10^9$ $m^3$ of natural gas and around $7{,}300 \times 10^6$ t of oil.

Table 2: Calculated amounts of natural gas and oil accumulated in the individual source rocks of each country

| Model | GIIP | | | OIIP | | |
|---|---|---|---|---|---|---|
| | free | adsorbed | total | free | adsorbed | total |
| | ($10^9$ $m^3$) | | | ($10^6$ t) | | |
| DK_Bo | 10 | 168 | 178 | 1,247 | 3,147 | 4,394 |
| DK_Bryne | 89 | 4,132 | 4220 | 0 | 2,921 | 2,921 |
| D_Bo | 0 | 2 | 2 | 2 | 62 | 64 |
| D (Posidonia_min) | 0 | 2 | 2 | 22 | 29 | 50 |
| D (Posidonia_max) | 11 | 12 | 22 | 99 | 132 | 231 |
| NL_Posidonia | 26 | 13 | 40 | 94 | 43 | 137 |

The amounts of accumulated petroleum are given for the whole source rock layer (Figure 15).

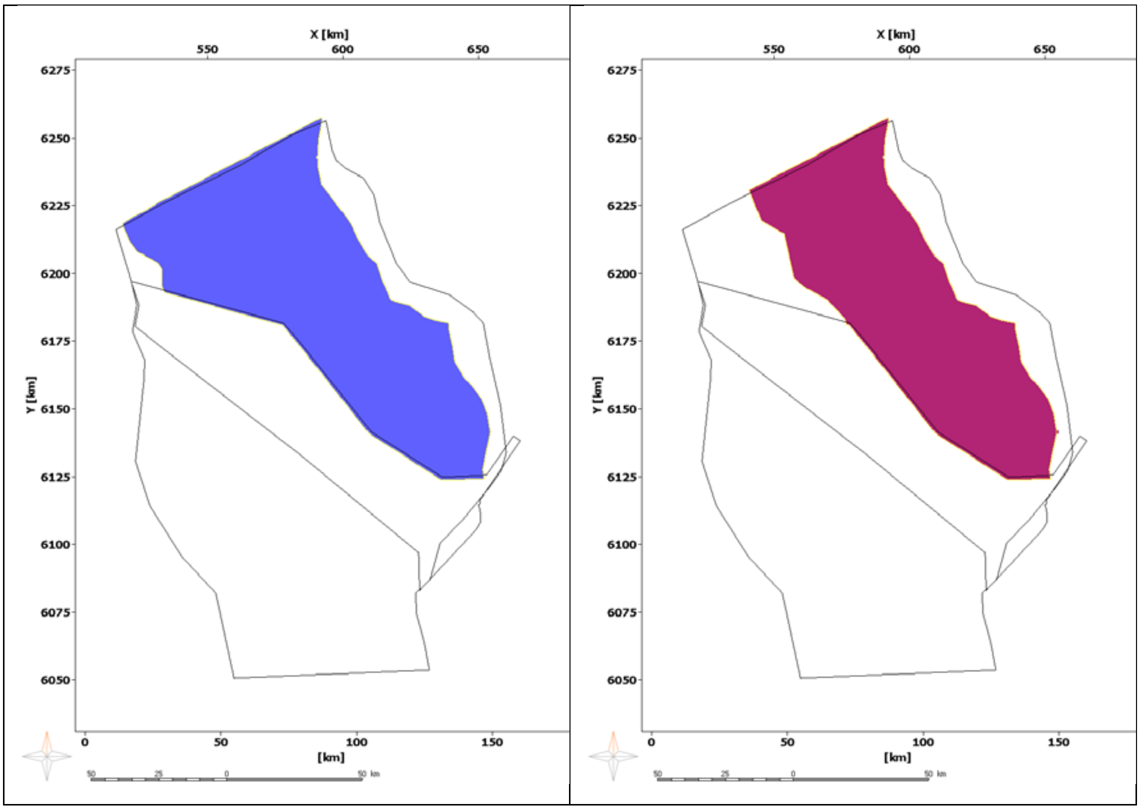

Figure 15: Extent of the Bo (left) and Bryne (right) source rocks in the 3D model.

### *4.2.2 Germany*

The Hot Shale (Bo) source rock in the German Central Graben accumulated around $2 \times 10^9$ $m^3$ of natural gas and around $64 \times 10^6$ t of oil. The amounts of free oil and gas are much smaller than the respective amounts of their adsorbed phases (Table 2). The extent of the German Bo source rock is much smaller than in the Danish North Sea and its thermal maturity is lower. Therefore, the amounts of oil and gas are significantly lower than in the Danish North Sea.

The extent of the Lower Jurassic Posidonia source rock in the German Central Graben is not well known. Therefore, we modelled two scenarios with a minimum and a maximum extent, respectively. The figures for natural gas lie between $2 \times 10^9$ and $22 \times 10^9$ $m^3$ and for oil between $50 \times 10^9$ and $231 \times 10^9$ t of oil.

Together, both source rocks accumulated up to $24 \times 10^9$ $m^3$ of natural gas and up to $295 \times 10^6$ t of oil (Figure 16).

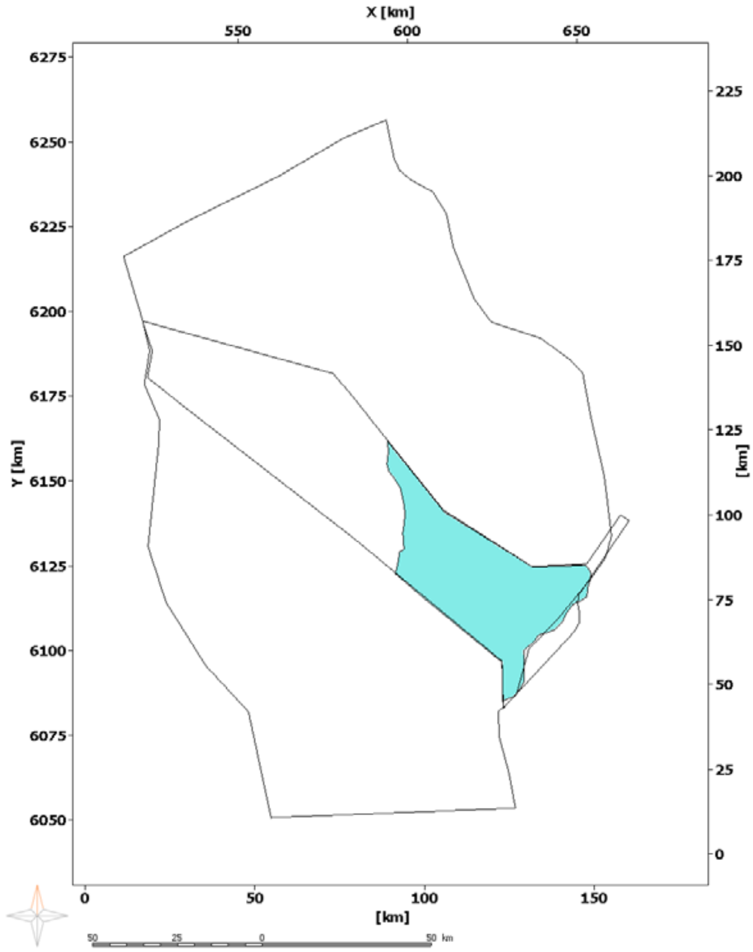


Figure 16: The Hot Shale (Bo) and Posidonia source rocks are mainly located in the German Central Graben.

### *4.2.3 Netherlands*

The Lower Jurassic Posidonia source rock in the Dutch Central Graben is restricted to the southernmost part of the study area (Figure 17). The values for natural gas are around $40 \times 10^9$ m$^3$ and for oil around $138 \times 10^9$ t of oil (Table 2).

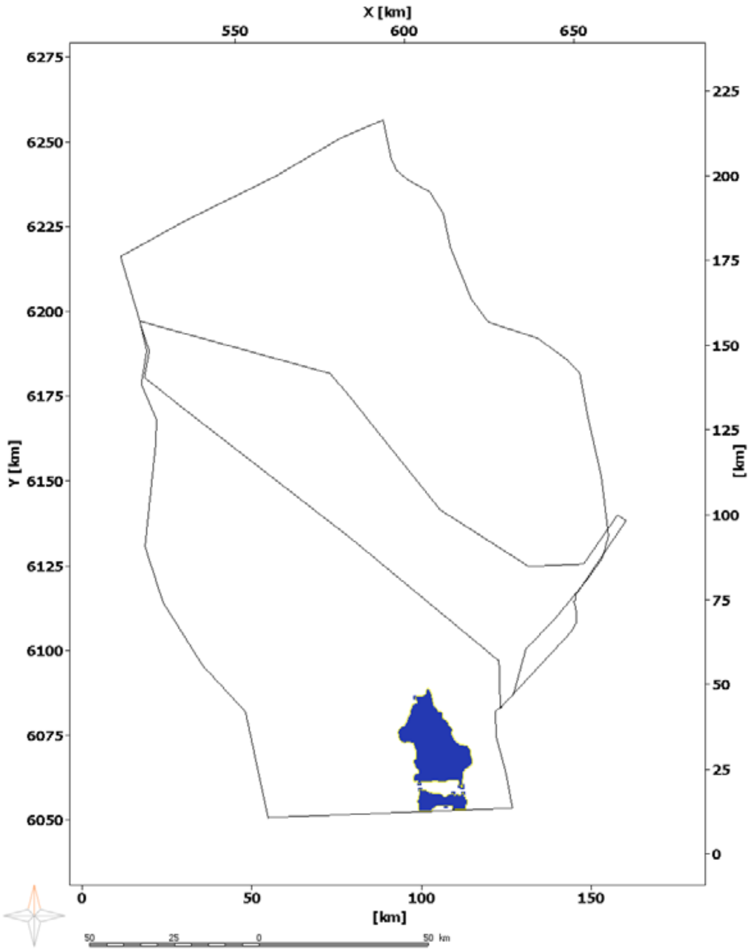


Figure 17: The Dutch Posidonia source rock is only present in the southern Dutch Central Graben.

## 4.3 Conclusions

The model presented here is the first publicly presented 3D basin and petroleum system model across the Danish, German and Dutch Central Graben area. It was built in close cooperation between the GARAH and 3DGEO-EU projects within the Geo-Energy theme of GeoERA. It serves as a pilot-study to identify cross-border issues on horizon correlation and high quality horizon grids are expected to be delivered at the end of the 3DGEO-EU project.

The cross-border model covers the Danish, German and Dutch Central Graben and its surrounding flanks, incorporating their distinct geological evolution. The model includes several of Central Europe's most prolific petroleum source rocks and captures their regional differences in maturity and quality. For these source rock layers in-place (unconventional) hydrocarbon resources were assessed. In an additional work package of the GARAH project the conventional resources will be assessed utilizing and refining the 3D model.

For the unconventional assessments, sensitivity tests were carried out. Two heat flow evolution scenarios were compared, showing a better fit of the default heat flow scenario than the alternative scenario. Furthermore, the two parameters, critical oil saturation and sorption capacity, were examined regarding their influence on the amount of retained petroleum (in-place resources). These tests showed that varying critical oil saturation had no significant effect on the amount of retained petroleum. However, reducing sorption capacity of oil resulted in up to 34 % less adsorbed oil, which is nearly counter-balanced by the amount of free oil in the pore space. Thus, the total amount of retained oil was only 4 % less. Yet, to a certain extent this comes at the expense of retained gas, which decreased by around 8 %.

The largest in-place amount of natural gas is assessed for the Danish Middle Jurassic Bryne Fm ($4{,}100 \times 10^9$ $m^3$) and the largest in-place oil resources were found for the Upper Jurassic Bo source rock ($4{,}400 \times 10^6$ t). The amounts of oil and natural gas in the Posidona Shale Fm is one to two orders of magnitude lower. The total amount of petroleum in-place for the whole modelled area is around $7{,}700 \times 10^6$ t for oil and around $4{,}500 \times 10^9$ $m^3$ for natural gas.

Uncertainties in the 3D model are not evenly distributed, basically due to varying data coverage and density in the three modelled sectors of Denmark, Netherlands and Germany. However, the 3D model can be further refined for more detailed studies with higher model resolution, e.g. with focus on smaller structural areas or on specific source rock or reservoir layers.

Additionally, the 3D basin and petroleum system model is not limited to petroleum assessments, but can be utilized for other studies, where basin and temperature evolution are critical for the 3D subsurface geological and petrophysical assessment e.g. within utilisation of geothermal energy or underground storage sites.

## 5 LITERATURE

Abdul Fattah, R., Verweij, J.M., Witmans, N. & Ten Veen, J.H. (2012a) Reconstruction of burial history, temperature, source rock maturity and hydrocarbon generation in the northwestern Dutch offshore. Netherlands Journal of Geosciences, 91, 535–554.

Abdul Fattah, R., Verweij, J.M., Witmans, N. & Ten Veen, J.H. (2012b) 4D Basin Modelling of the Broad Fourteens Basin and Offshore West Netherlands Basin; Erosion and Heat Flow Reconstruction and ist Influence on Temperature, Maturity and Hydrocarbon Generation. TNO Report 2012 R10670. Netherlands Institute of Applied Geosciences (TNO), Utrecht, The Netherlands.

Arfai, J. & Lutz, R. (2017) 3D basin and petroleum system modelling of the NW German North Sea (Entenschnabel). In *Petroleum Geology of NW Europe: 50 Years of Learning – Proceedings of the 8th Petroleum Geology Conference* (eds Bowman, M. & Levell, B.), doi: 10.1144/PGC8.35.

Bonté, D., Smit, J., Abdul Fattah, R., Nelskamp, S., Cloetingh, S., van Wees, J-D. (2020) Quantifying the late- to post-Variscan pervasice heat flow, central Netherlands, Southern Permian Basin. Marine and Petroleum Geology, 113, 104118.

Doornenbal, H., den Dulk, M., Middelburg, H., 2019. A generalized 3D depth model of the Entenschnabel region. Project number: GeoE.171.005, p. 21, https://geoera.eu/3DGEO-files/3DGEO-EU-D3.2-Supporting-Document.pdf.

Doornenbal, J.C. & Stevenson, A.G. (Eds) (2010): Petroleum Geological Atlas of the Southern Permian Basin Area. EAGE Publications b.v., Houten, 342 pp.

Hantschel, T. & Kauerauf, A.I. (eds. 2009) Fundamentals of Basin and Petroleum Systems Modelling. Springer, Berlin.

Lutz, R., Littke, R., Gerling, P., Bönnemann, C. (2004) 2D numerical modelling of hydrocarbon generation in subducted sediments at the active continental margin of Costa Rica. Marine and Petroleum Geology 21, 753-766.

Pepper, A.S.& Corvi, P.J. (1995) Simple kinetic models of petroleum formation. Part I: oil and gas from kerogen. Marine Petroleum Geology, 12, 291–319.

Peters, K.E., Curry, D.J., Kacewicz, M., (2012) An overview of basin and petroleum system modeling; definitions and concepts. AAPG Hedberg Series 4, 1-17.

Pluymaekers, M.P.D., Doornenbal, J.C., Middelburg, H. (2017) Velmod-3.1. TNO report TNO 2017 R11014, 67pp.

Sweeney, J.J. & Burnham, A.K. (1990) Evaluation of a simple model of vitrinite reflectance based on chemical kinetics. American Association of Petroleum Geologists Bulletin, 74, 1559–1570.

Ten Veen, J.H., Van Gessel, S. & Den Dulk, M. (2012) Thin-and thickskinned salt tectonics – Examples from the Dutch North Sea. Netherlands Journal of Geosciences, 91, 447–464.

Thöle, H., Jähne-Klingberg, F., Bense, F., Doornenbal, H., den Dulk, M., Britze, P., 2019. State of the Art Report. Project number: GeoE.171.005, p. 50, https://geoera.eu/3DGEO-files/3DGEO-EU-D3.1-State-of-the-art-report.pdf.

Van Wees, J.D., van Bergen, F., David, P., Nepveu, M., Beekman, F., Cloetingh, S., Bonté, D., (2009) Probabilistic tectonic heat flow modeling for basin maturation: Assessment method and applications. Marine and Petroleum Geology 26, 536-551 doi: 10.1016/j.marpetgeo.2009.01.020.

Verweij, J.M., Souto Carneiro Echternach, M., Witmans, N. & Abdul Fattah, R. (2011) Reconstruction of basal heat flow, surface temperature, source rock maturity, and hydrocarbon generation in salt-dominated Dutch Basins. In: Peters, K., Curry, D. & Kacewicz, M. (eds) Basin and Petroleum System Modelling. American Association of Petroleum Geologists, Hedberg Series, 4, 175–195.

Verreussel, R.M.C.H., Bouroullec, R., Munsterman, D.K., Dybkjær, K., Geel, C.R., Houben, A.J.P., Johannessen, P.N., Kerstholt-Boegehold, S.J., 2018. Stepwise basin evolution of the Middle Jurassic–Early Cretaceous rift phase in the Central Graben area of Denmark, Germany and The Netherlands. Geological Society, London, Special Publications 469(1), 305-340, doi: 10.1144/sp469.23.

Wygrala, B.P. (1989) Integrated study of an oil field in the southern Po basin,northern Italy. PhD thesis, Köln University, Jülich Research Centre, Jülich, Germany.

# 6 APPENDICES

Appendix 1: Petroleum System Model - Parameters Spreadsheet.

Appendix 2: Heat flow input maps for the alternative heat flow model. The heat flow values were extended beyond the study area to fill the whole rectangular map for simulation purposes.

Appendix 3: 1D models at well locations illustrationg the fit between measured and calculated vitrinite reflectance data.

# Appendix 1

| GARAH 3D Petroleum System Model (input parameters for PetroMod) | Data availability | | |
|---|---|---|---|
| **Present-day input** | **TNO** | **GEUS** | **BGR** |
| Absolute ages of horizons | Absolute ages of horizons have to be defined together | | |
| Lithology | Generalized lithology based on unit/formation description - See excel | Generalized lithology based on unit/formation description | Generalized lithology from well reports |
| Facies maps | uniform | uniform | uniform |
| Fault surfaces (main faults in the study area) | Can provide major fault lines | Work needed to create consistent major faults | Schillgrund Fault, Mads Fault, boundary faults of Clemens Basin |
| **Paleo Geometry** | | | |
| Erosion events | Mid-Jurassic (Mid-Kimmerian), Upper Cretaceous (Subhercynian), Paleocene (Laramide) and MMU - See tectonostratigraphic chart | - Mid-Jurassic (Mid-Cimmerian)<br>- Late Cretaceous erosion<br>- MMU erosion | • Mid-Jurassic (Mid-Cimmerian)<br>• Late Cretaceous erosion<br>• MMU erosion |
| Erosion maps - Paleo thicknesses of eroded formations | Erosion estimates from previous 1D and 3D studies based on seismic data and present-day thicknesses | Estimated erosion based on seismic data and present day thicknesses | Estimated paleo thicknesses based on seismic data and calculated present day thicknesses in graben systems in the Entenschnabel area |
| Salt maps, intitial salt thicknesses, and salt activity during the geological periods | Paper Johan ten Veen 2012 NJG | Salt diapirs are based on Top Zechstein surface-grid including the salt polygons | Salt diapirs are included in the 3D model using the top Zechstein surface-grid including the salt polygons |
| **Boundary conditions** | | | |
| Heat flow data | Calculating new maps based on PetroMod model with PetroProp | Simple regional heat flow trends | Two areas with different heat flow trends |
| Palaeo water depths | Same PWD trends are used for our models | Simple regional PWD trend maps | Paleowater depth (PWD) based on PWD trends of adjacent areas (Verweij et al. 2009; Abdul Fattah et al. 2012) |
| **Calibration data** | | | |
| Vitrinite reflectance data | see table | more than 40 wells with VitRef data | 16 wells with vitrinte reflectance data |
| Tmax | see table | some wells with Tmax | 3 wells with Tmax |
| Temperature | see table | more than 40 wells with Temp data | 6 wells with temperature data |
| **Source rocks and their properties** | | | |
| Upper Jurassic (Clay deep, Kimmeridge, Lola FM) | not included in models until now | Late Jurassic- Early Cretaceous Farsund Fm; Kinetics: Pepper & Corvi (1995) | • HI 430 mgHC/gTOC<br>• TOC 8%<br>• Kinetics Vandenbroucke et al. (1999), TII North Sea<br>(uniform values) |
| Lower Jurassic (Posidonia Shale) | HI: 400, TOC: 6%, Kinetics: Pepper&Corvi TII(B) | Middle Jurassic Bryne Fm; Kinetics: Pepper & Corvi (1995) | • HI 400 mgHC/gTOC<br>• TOC 8%<br>• Kinetics Vandenbroucke et al. (1999), TII North Sea<br>(uniform values) |
| **Reservoir rocks** | | | |
| | Paleogene<br>Upper Cretaceous chalk<br>Upper Jurassic sands | Upper Cretaceous - Chalk Group<br>Jurassic sands | Upper Cretaceous - Chalk Group<br>Jurassic sands |

# Appendix 2

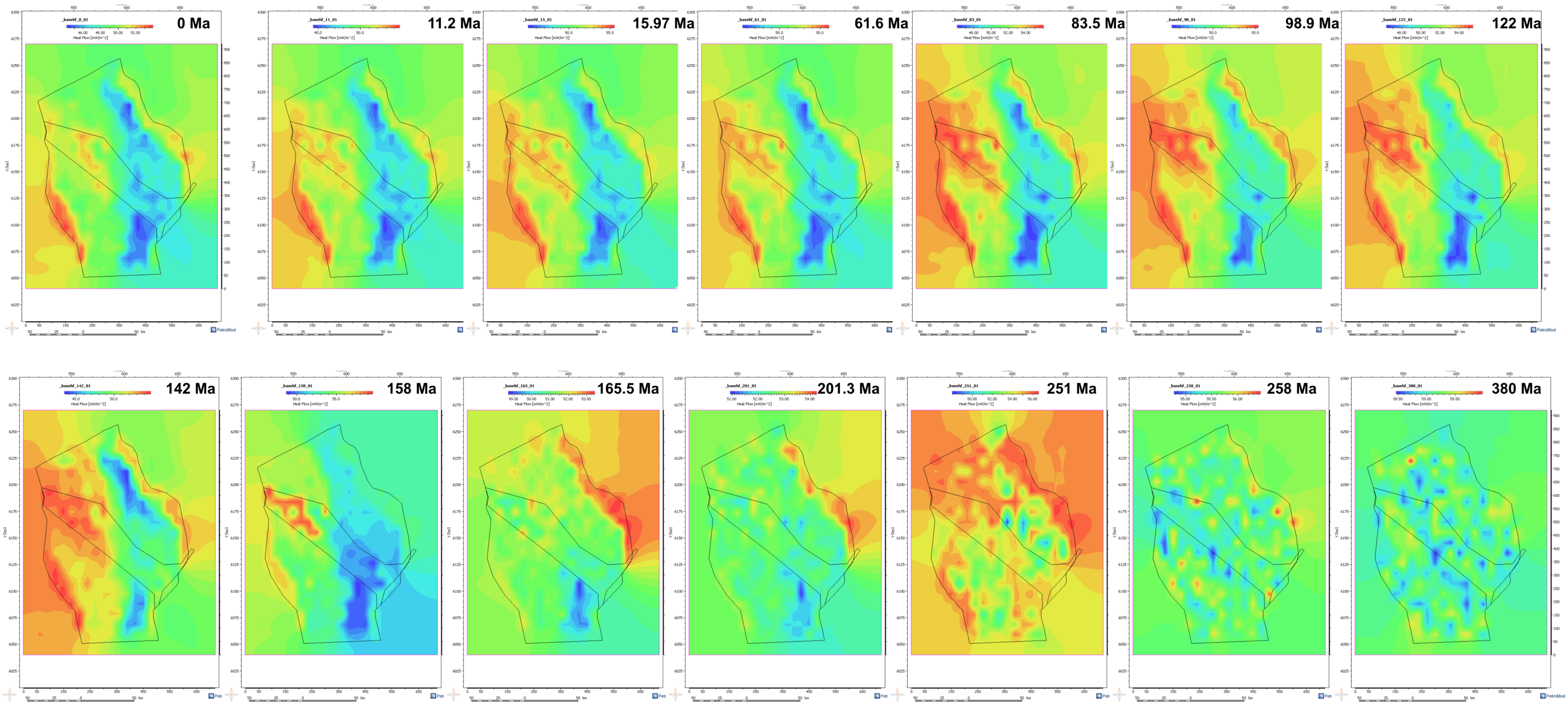
0 Ma
11.2 Ma
15.97 Ma
61.6 Ma
83.5 Ma
98.9 Ma
122 Ma
142 Ma
158 Ma
165.5 Ma
201.3 Ma
251 Ma
258 Ma
380 Ma

# Appendix 3
# Calibration default heat flow model

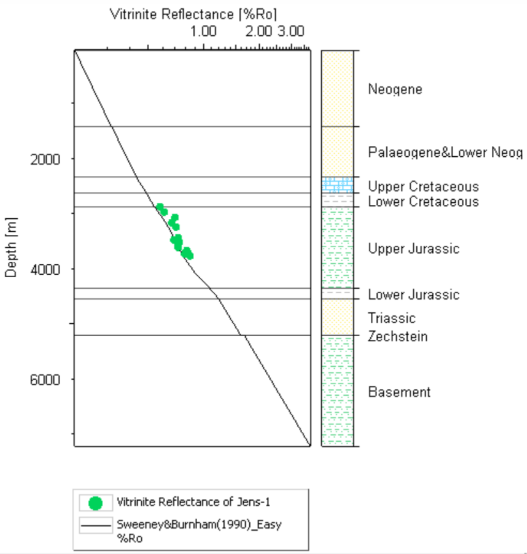


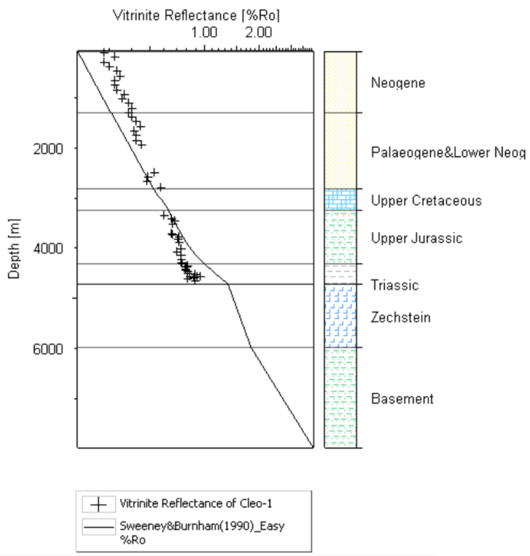


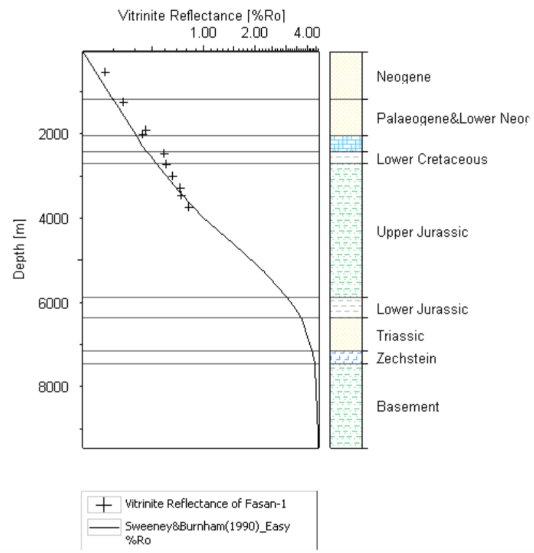


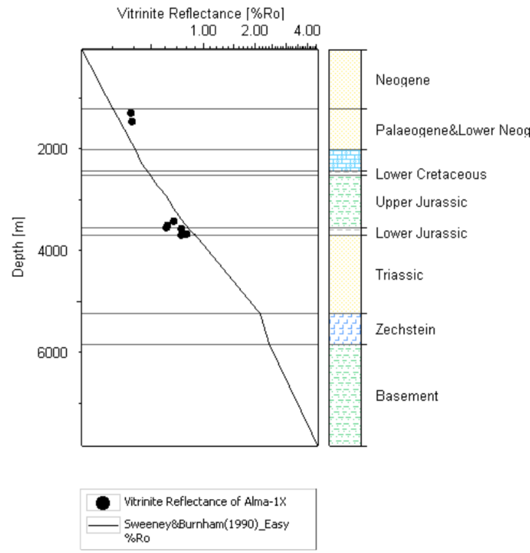


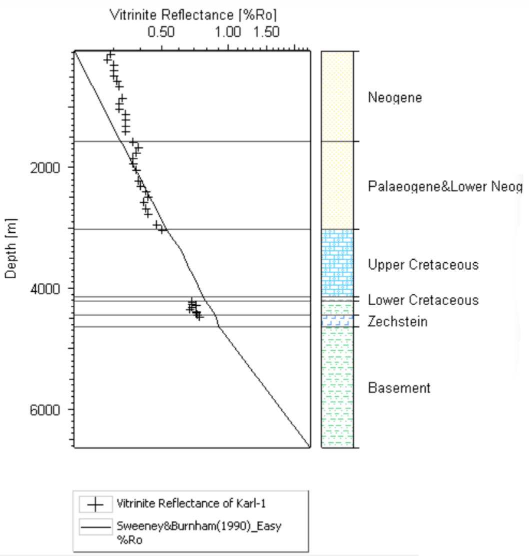


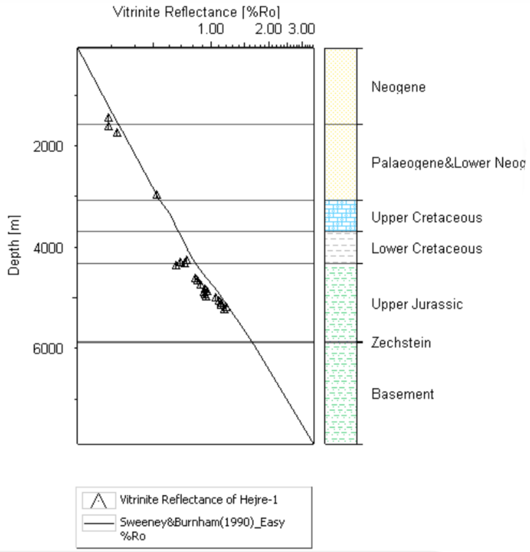


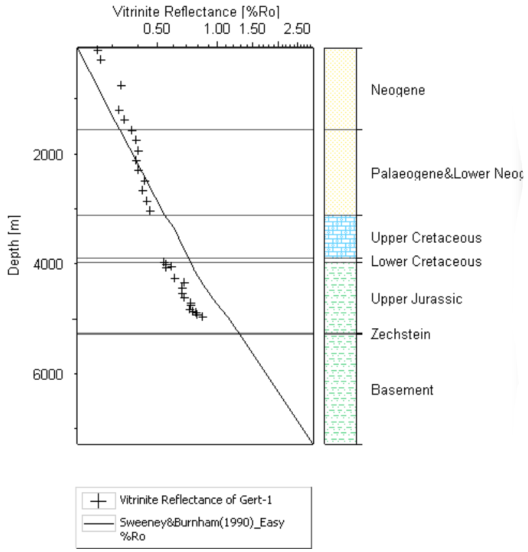


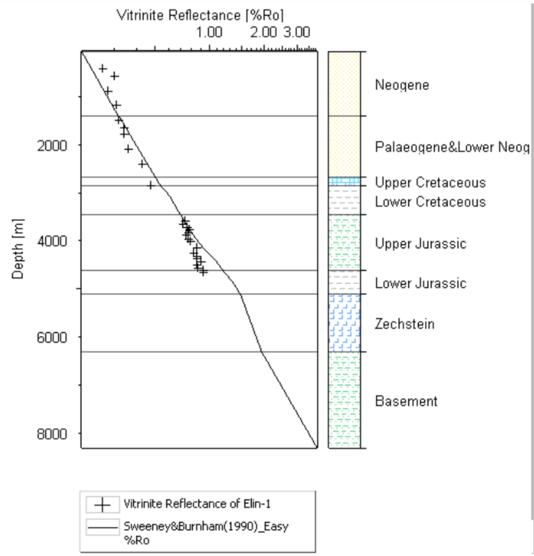

# Calibration default heat flow model

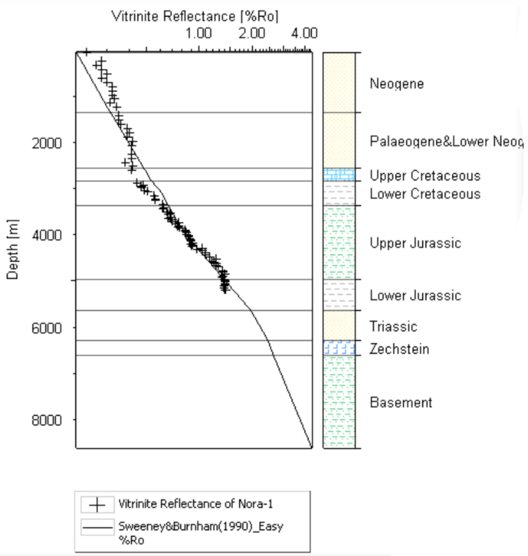


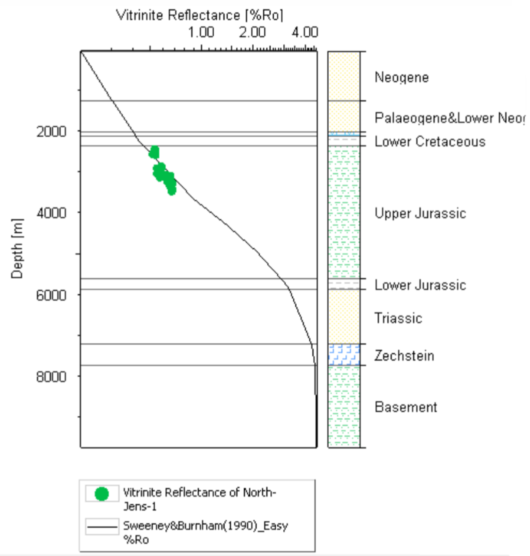


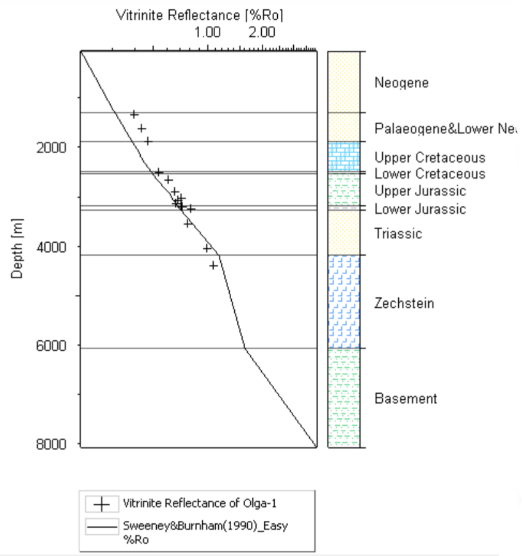


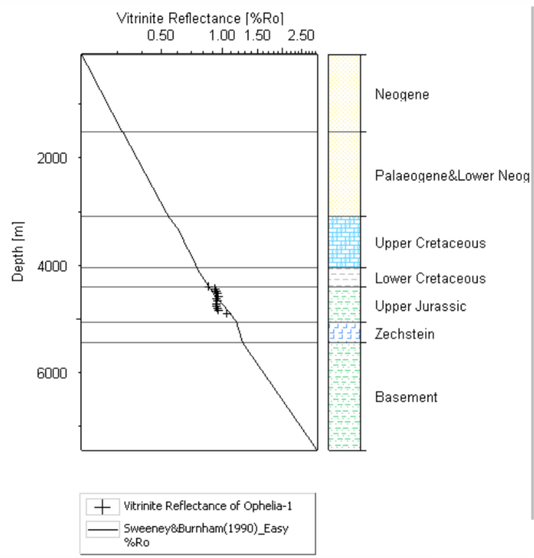


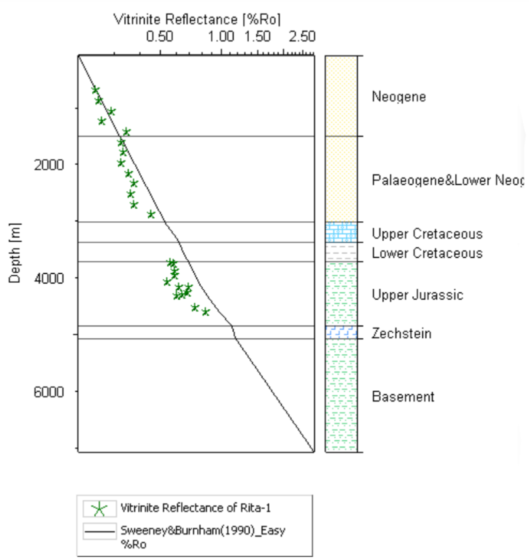


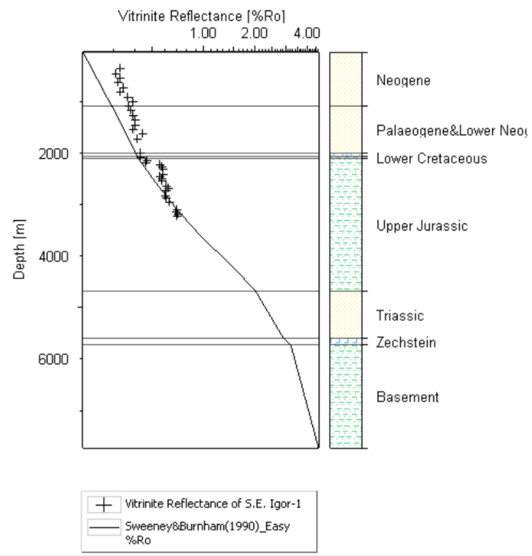


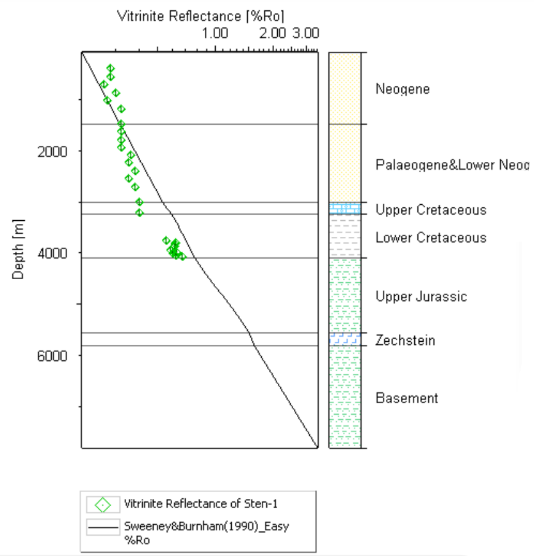


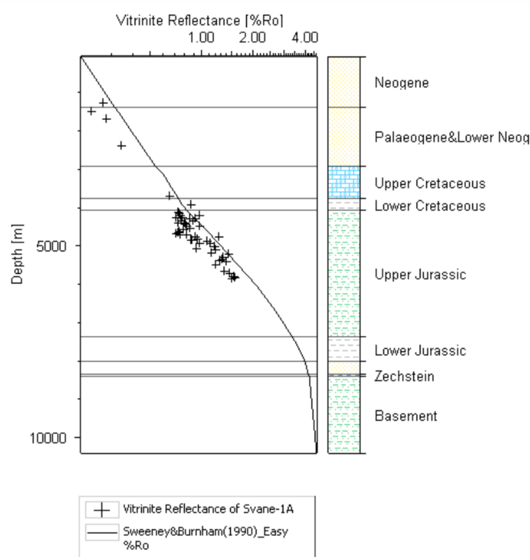

# Calibration default heat flow model

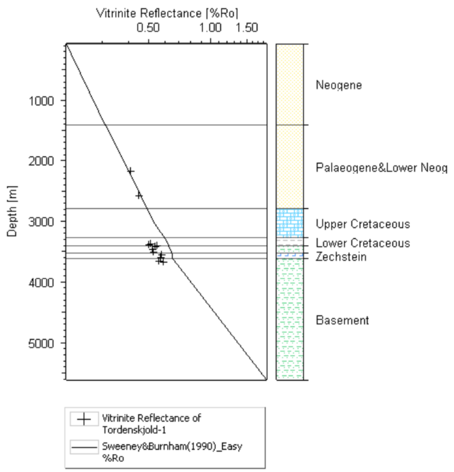

# Calibration default heat flow model

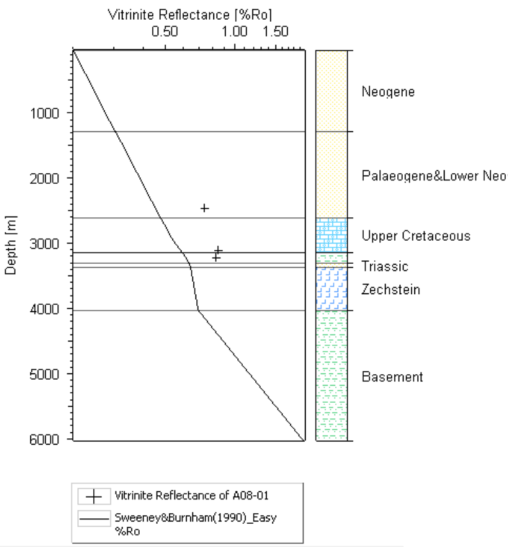


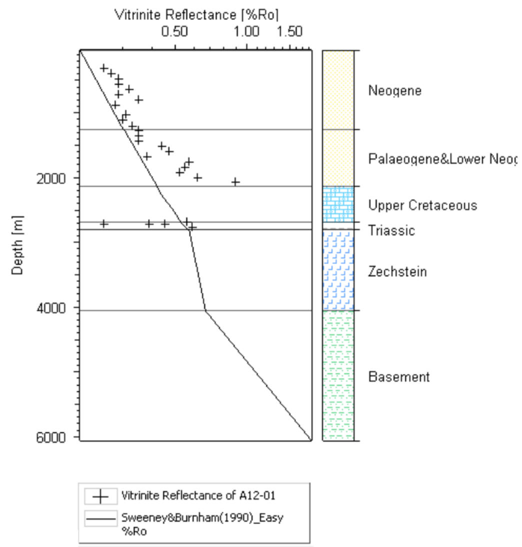


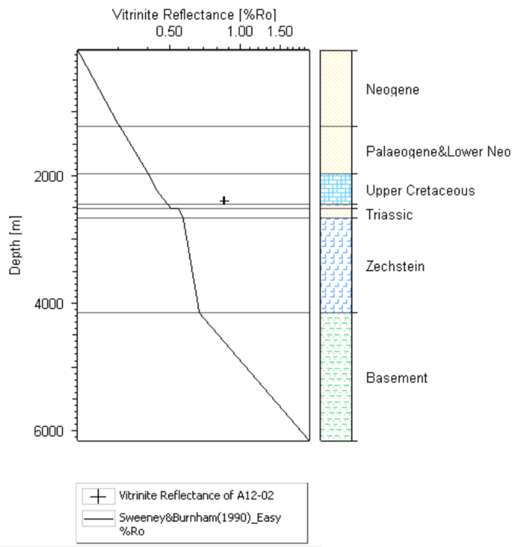


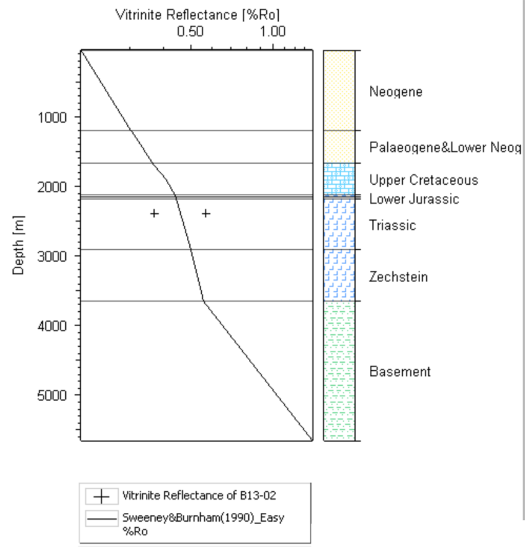


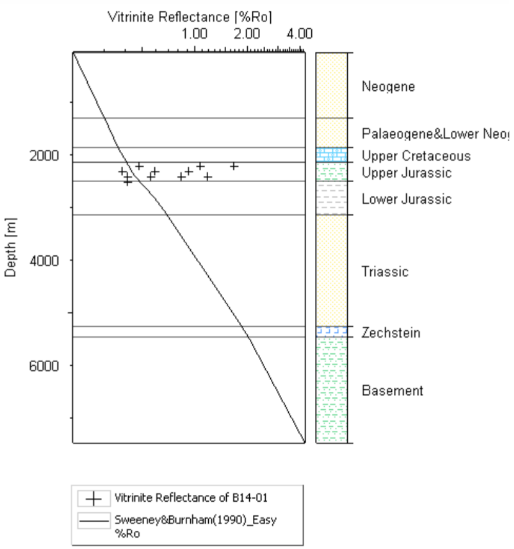


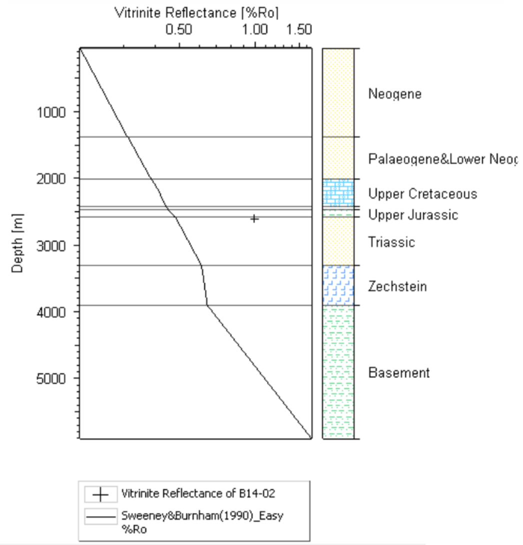


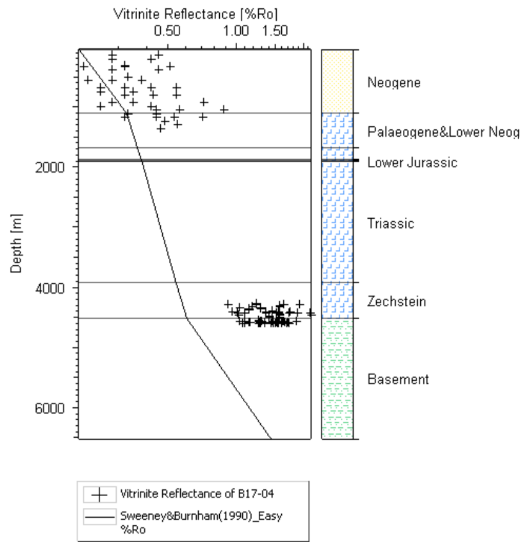


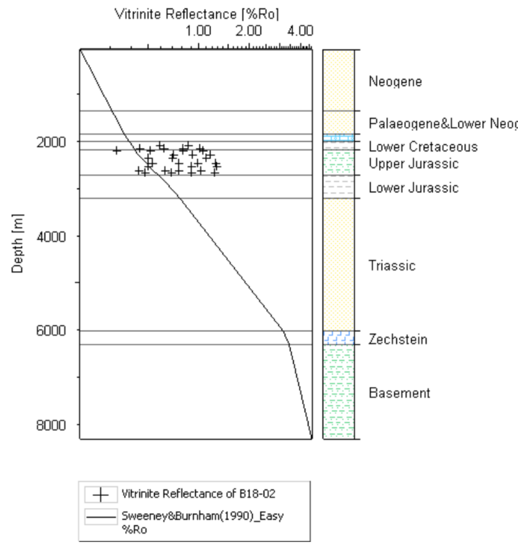

# Calibration default heat flow model

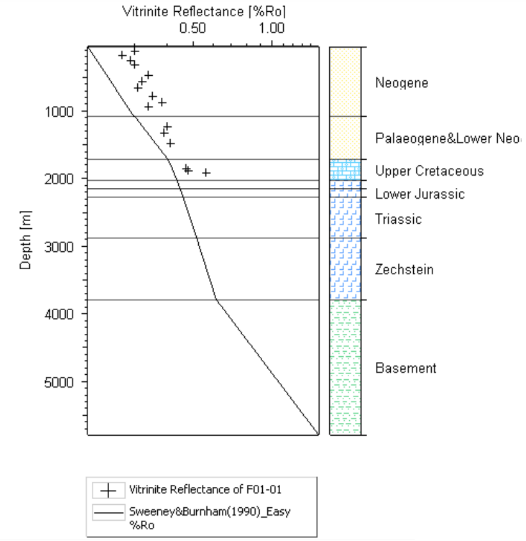


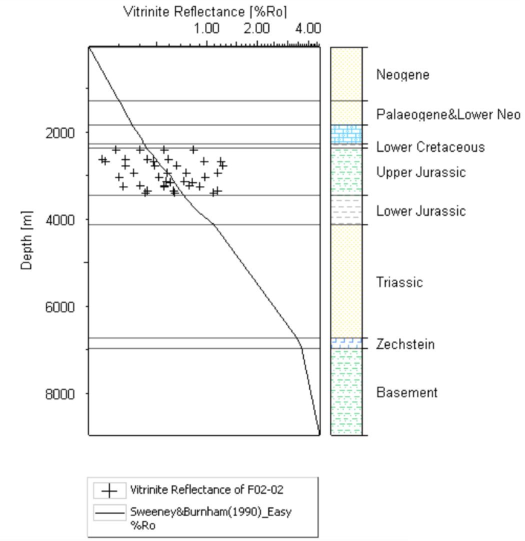


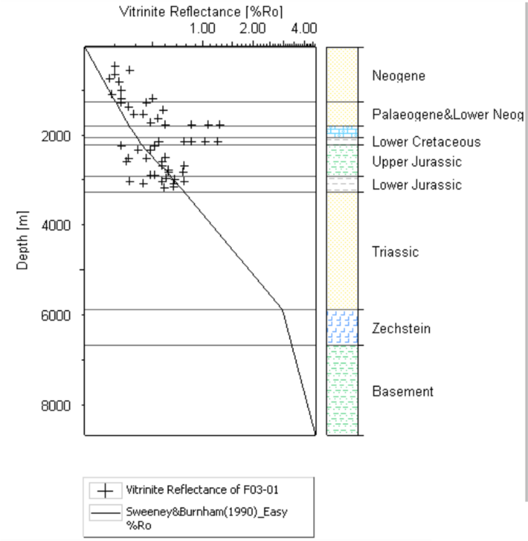


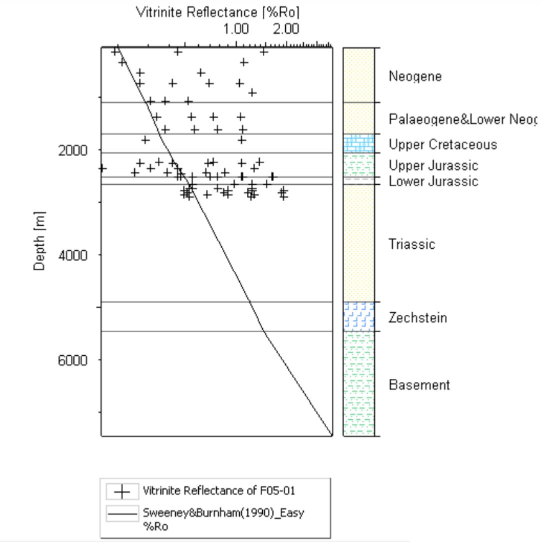


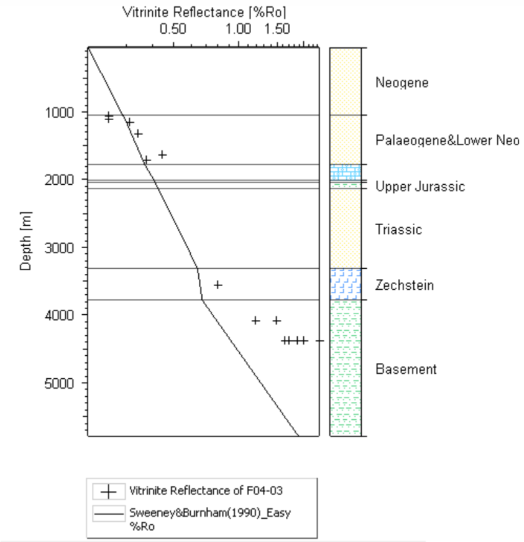


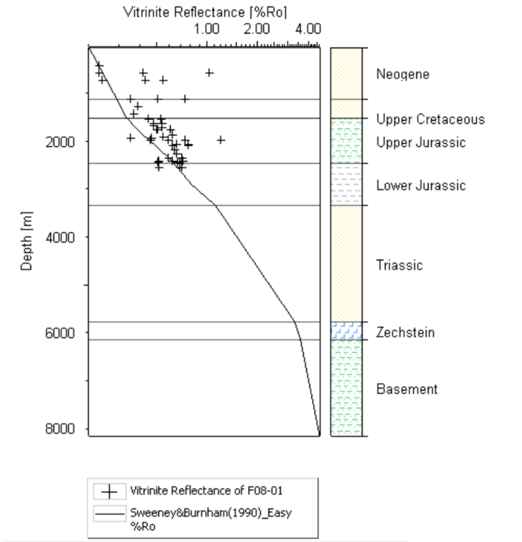


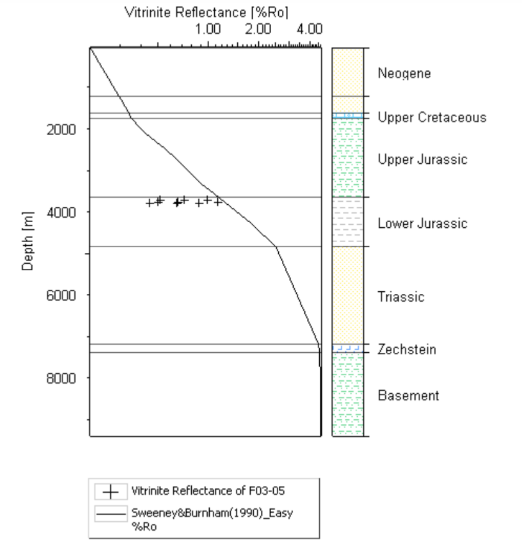

# Calibration default heat flow model

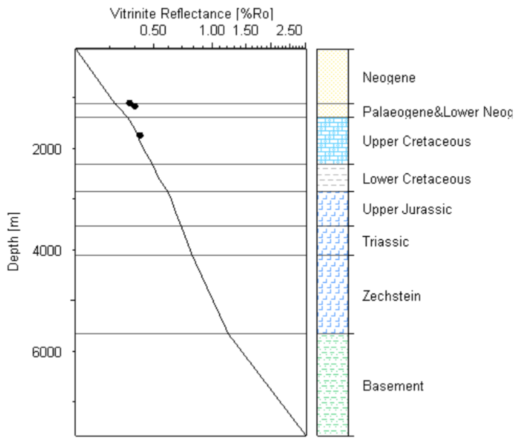


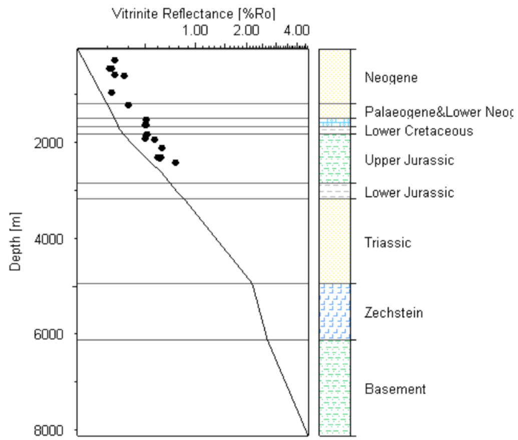


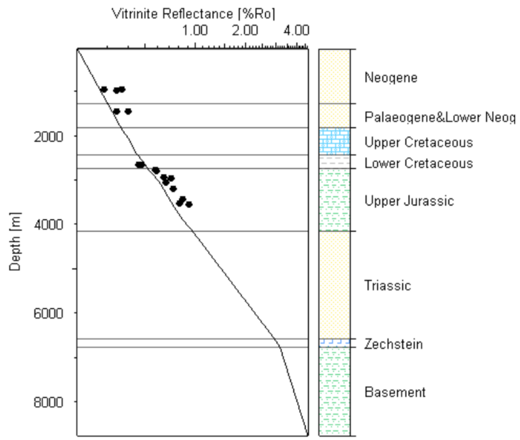


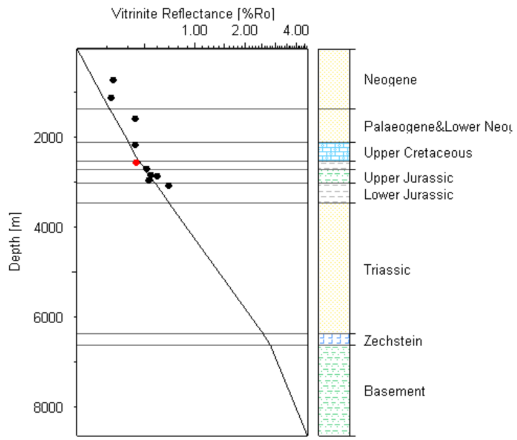


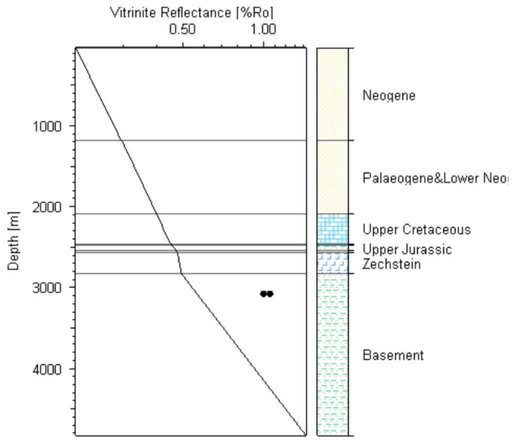


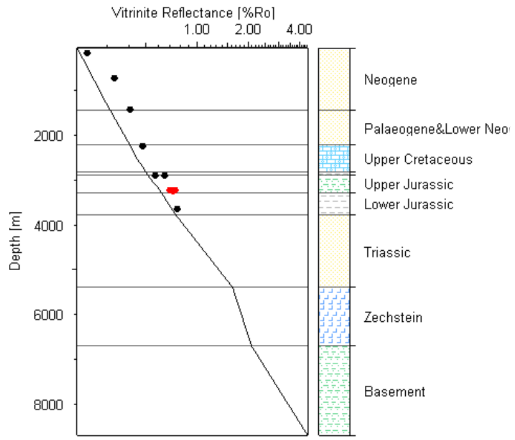


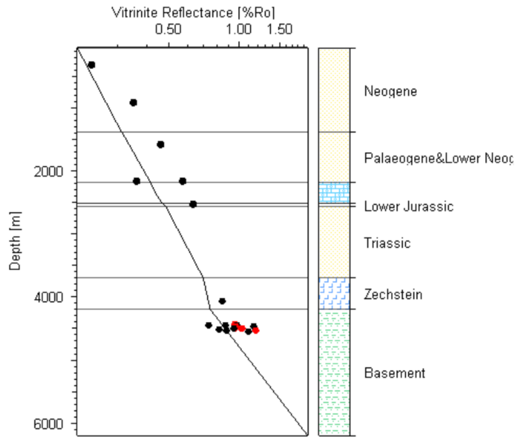


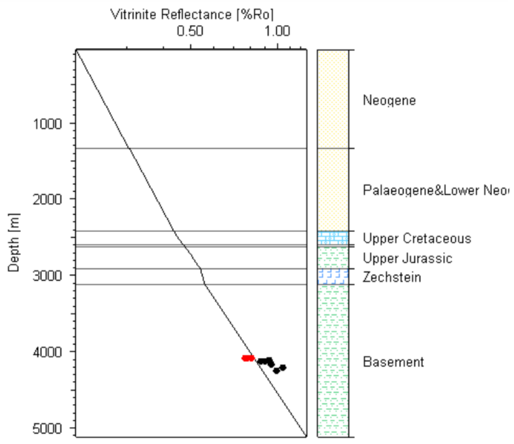

# Calibration default heat flow model

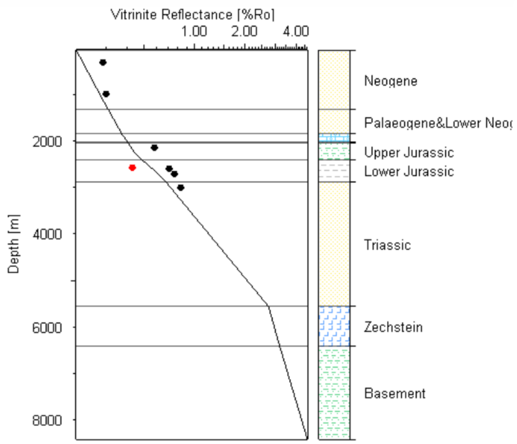


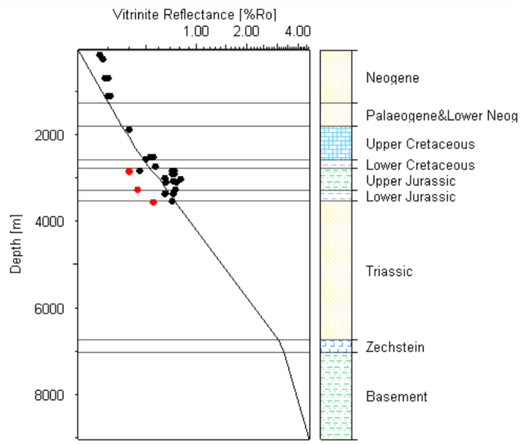


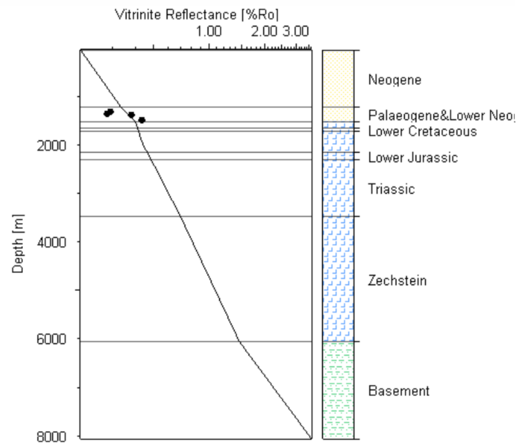


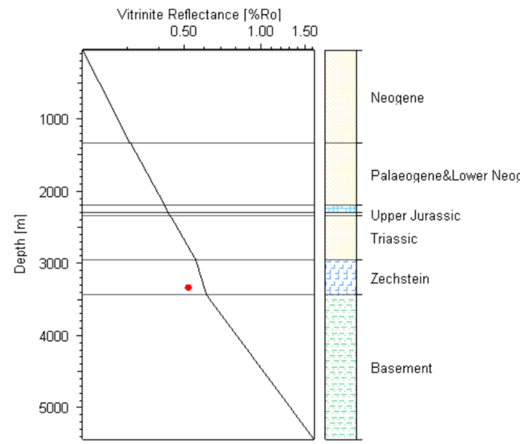


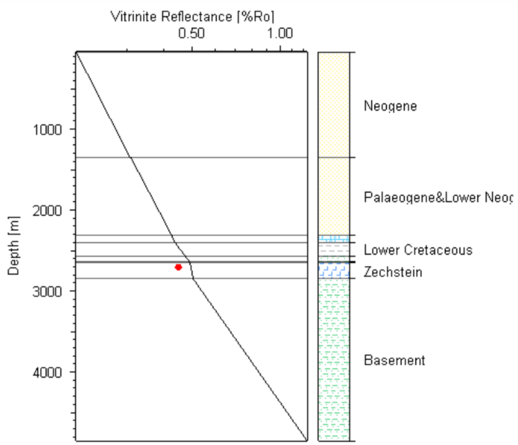


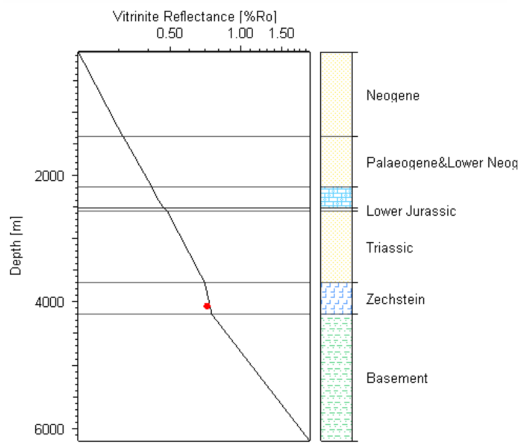


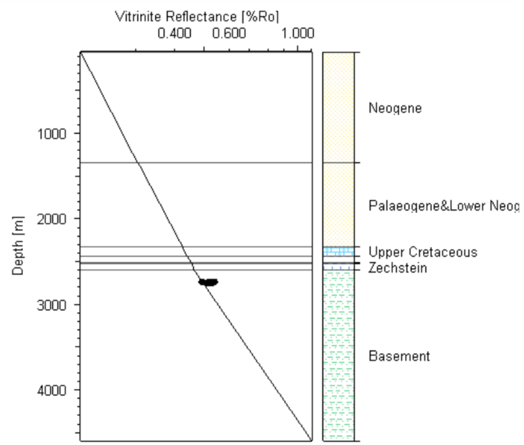


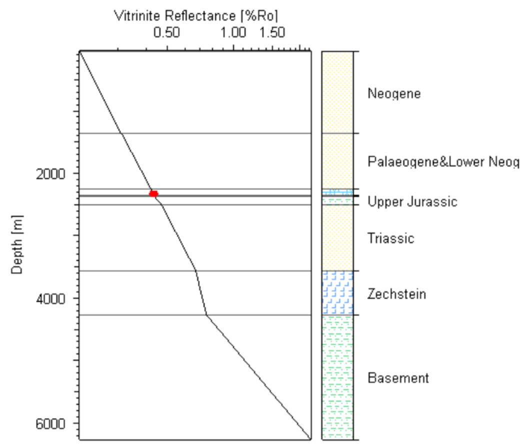

# Calibration alternative heat flow model

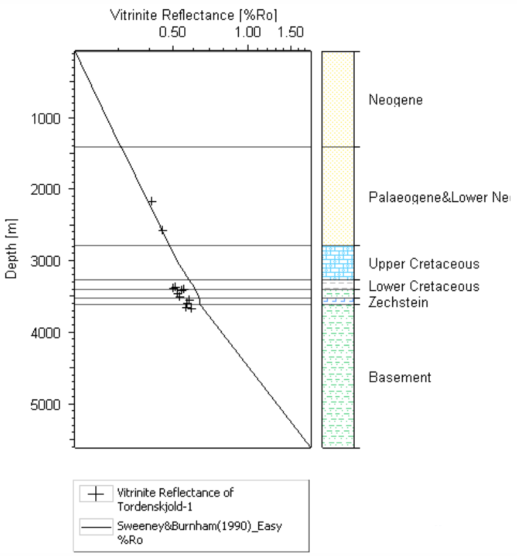


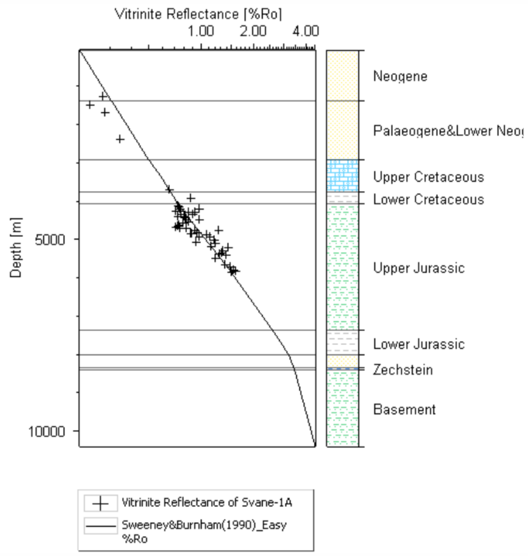


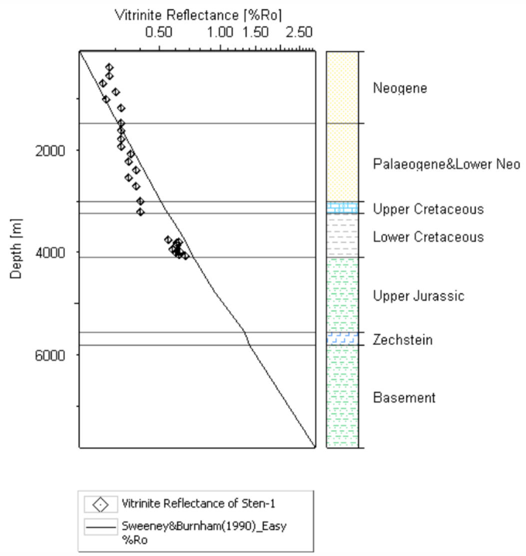


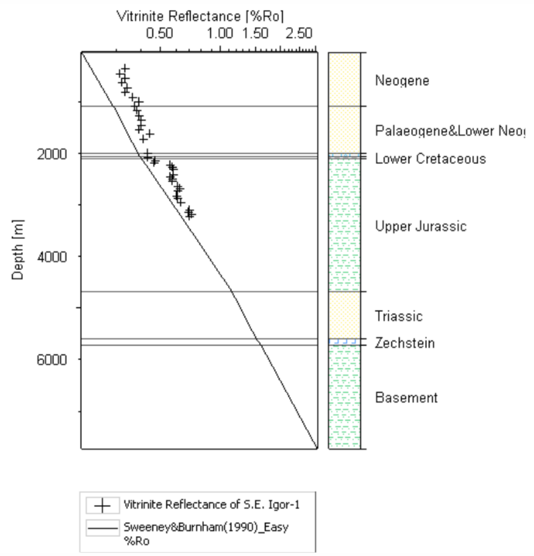


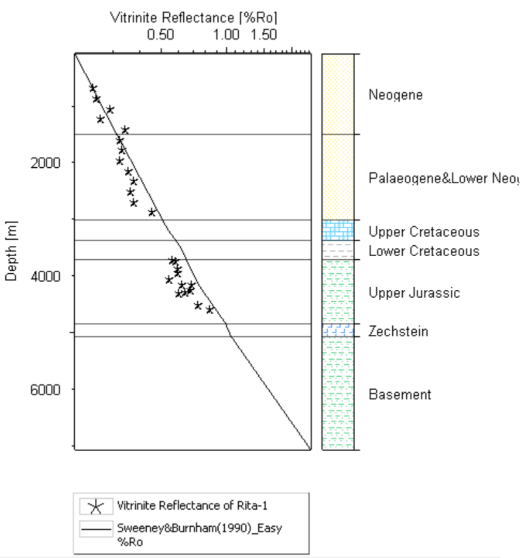


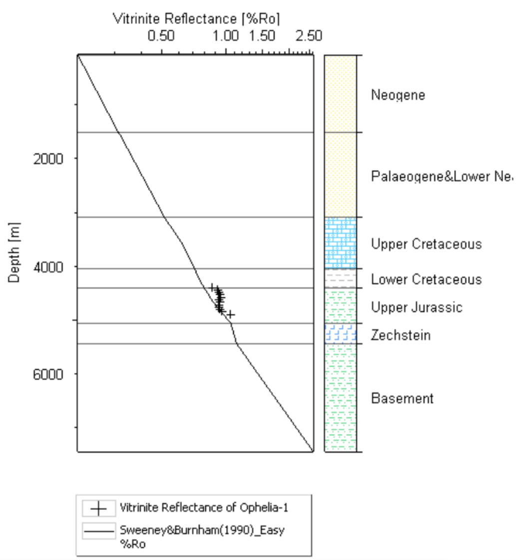


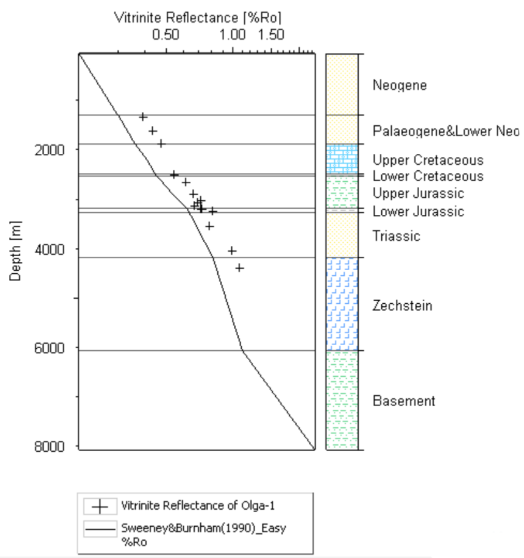


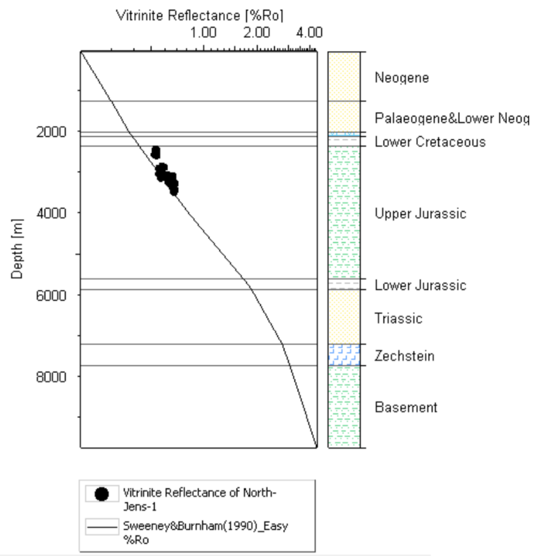

# Calibration alternative heat flow model

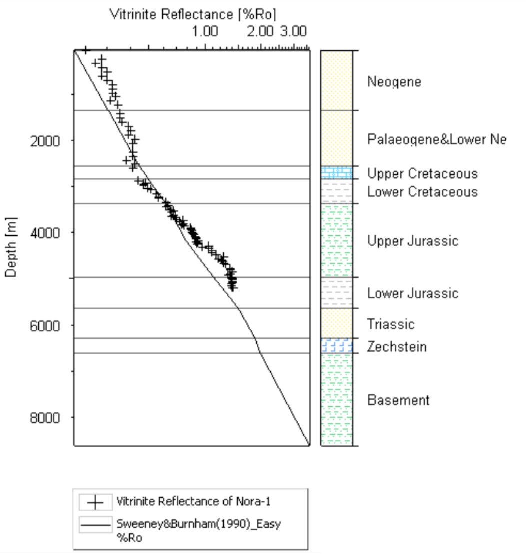


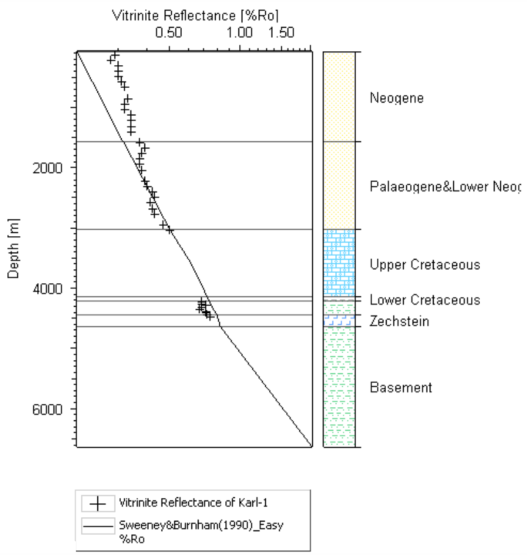


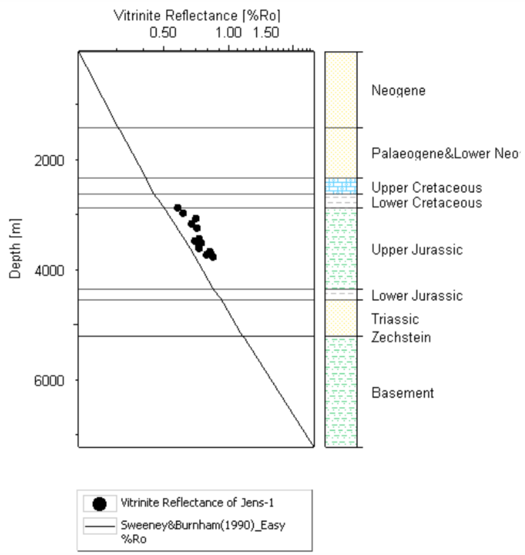


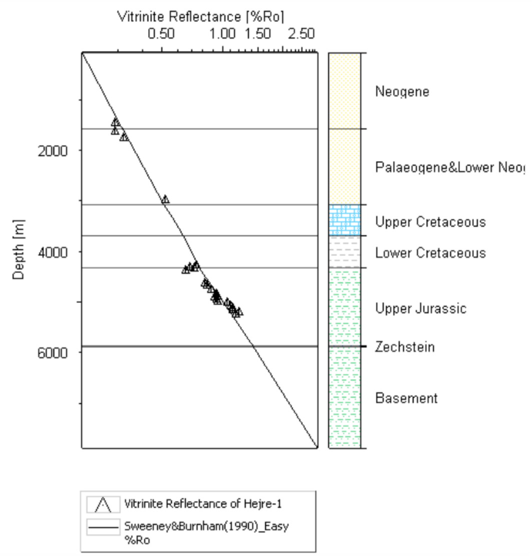


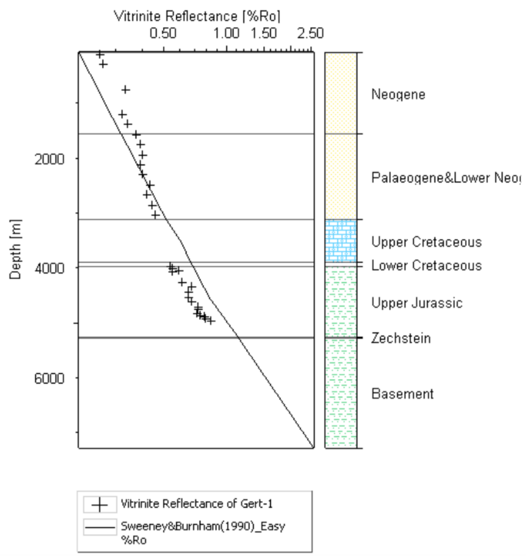


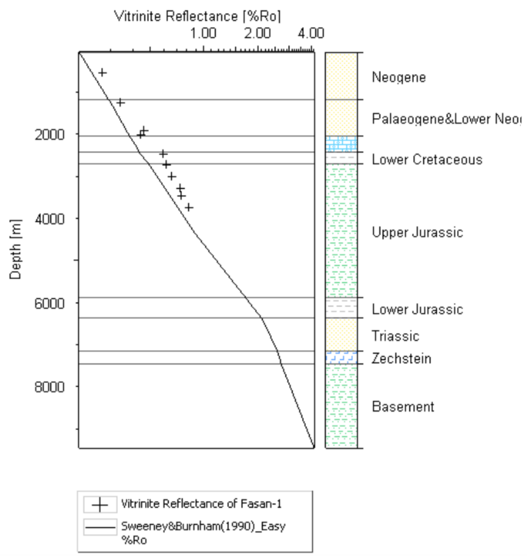


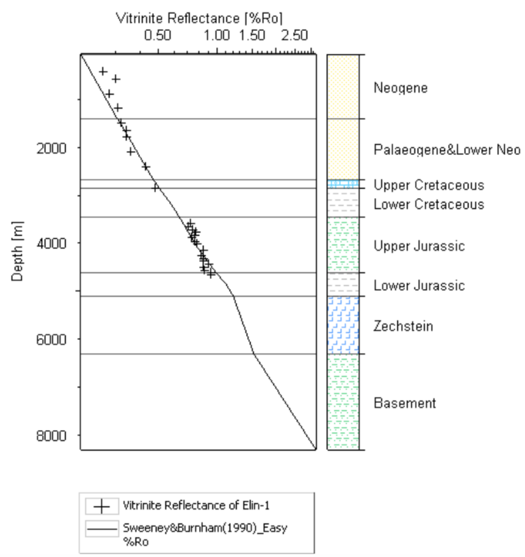


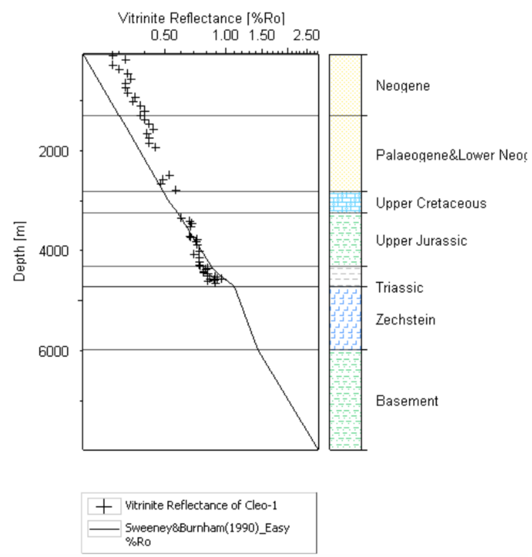

# Calibration alternative heat flow model

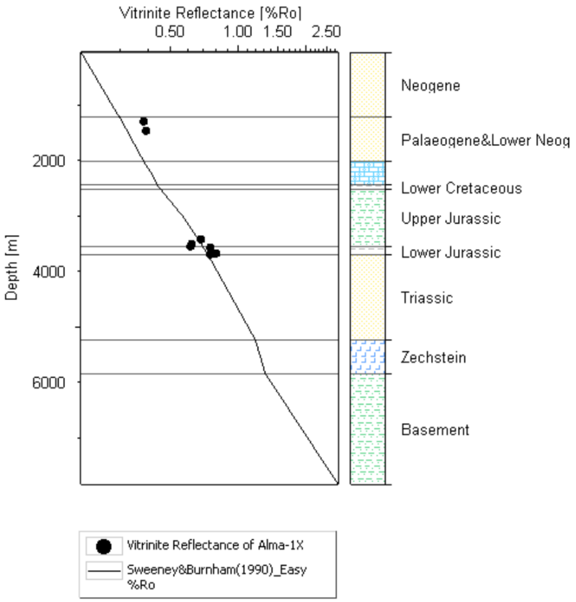

# Calibration alternative heat flow model

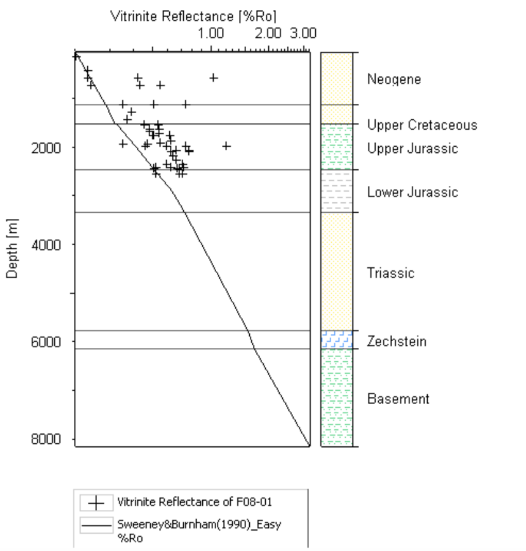


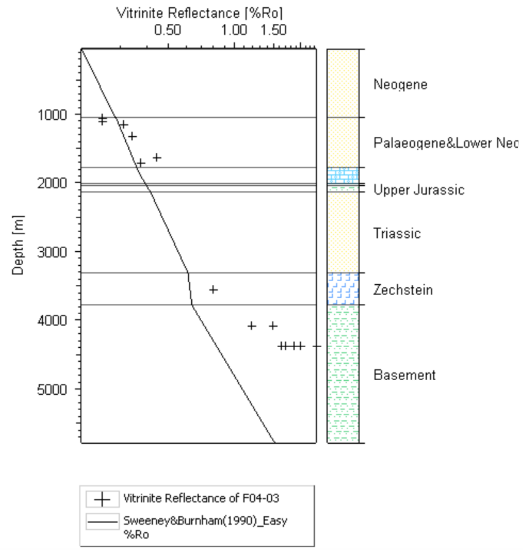


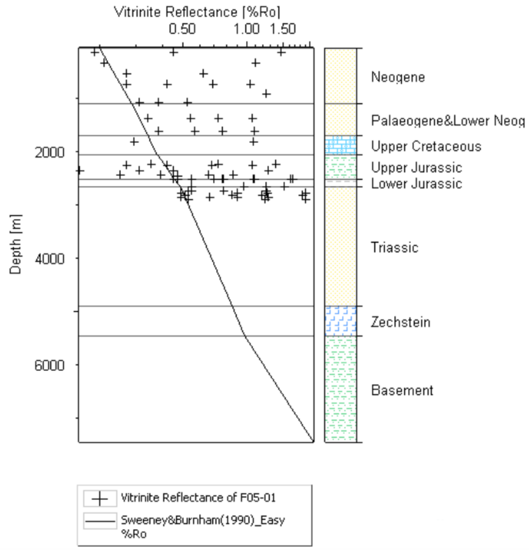


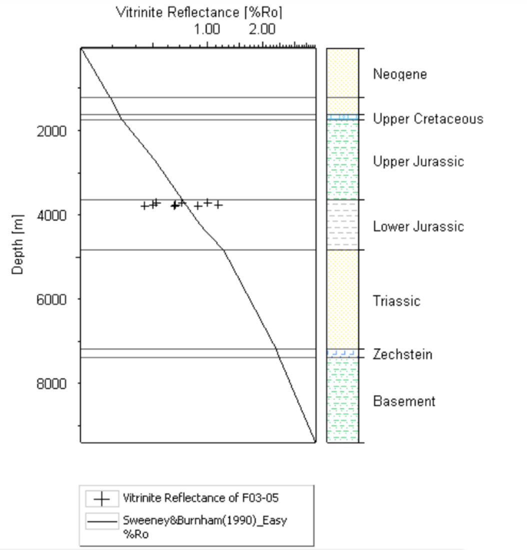


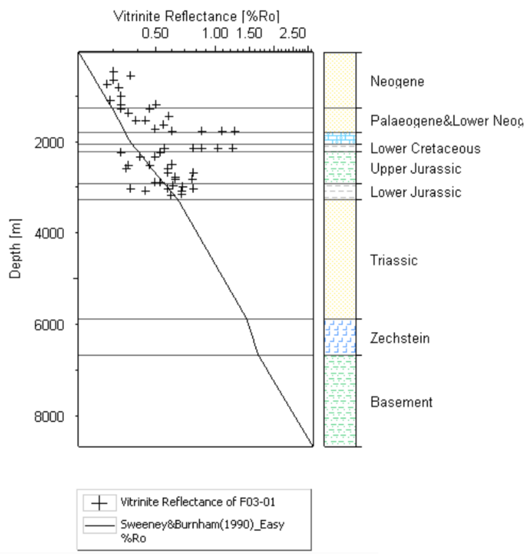


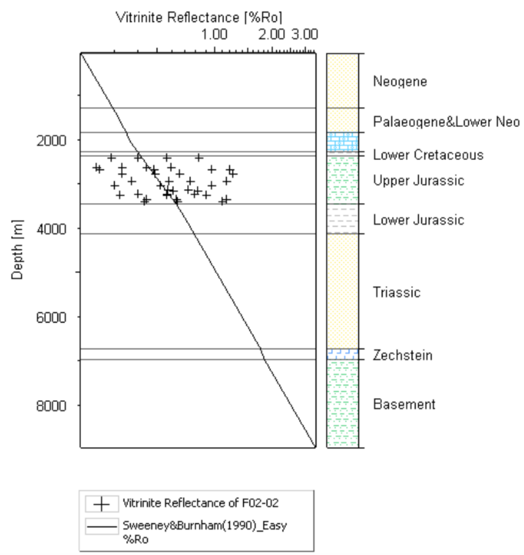


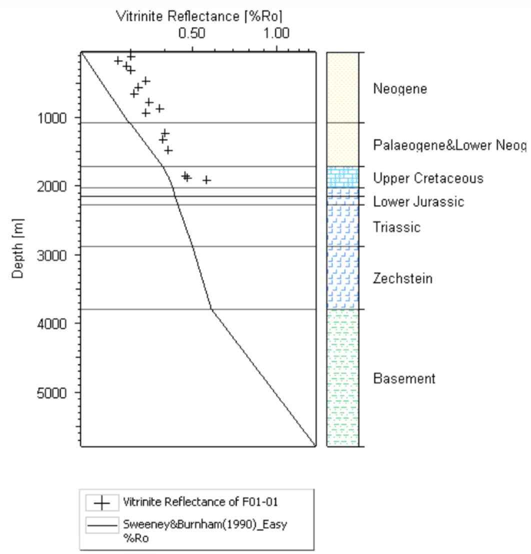


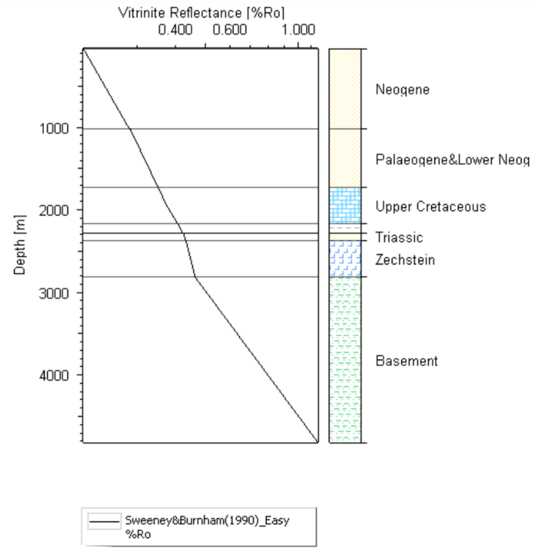

# Calibration alternative heat flow model

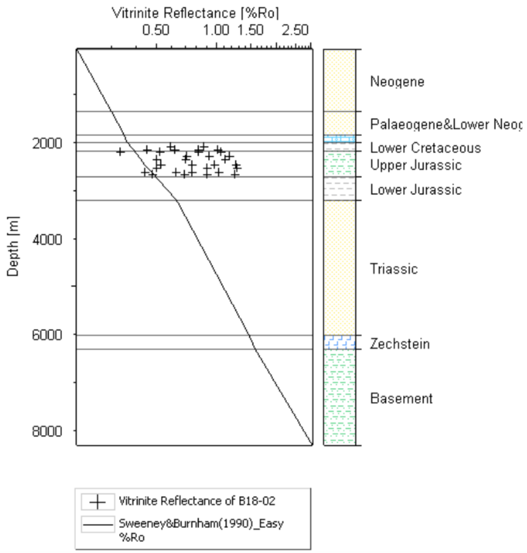


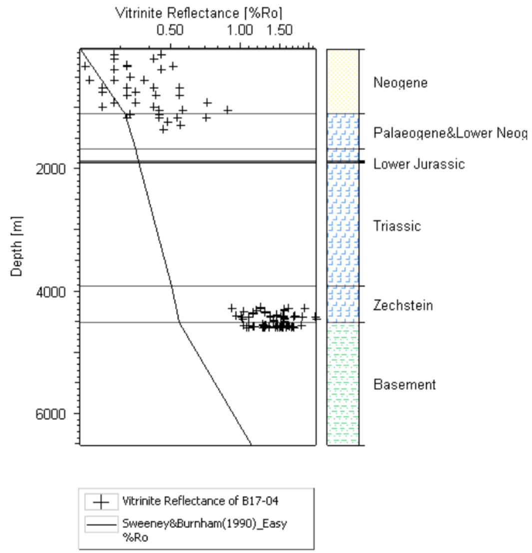


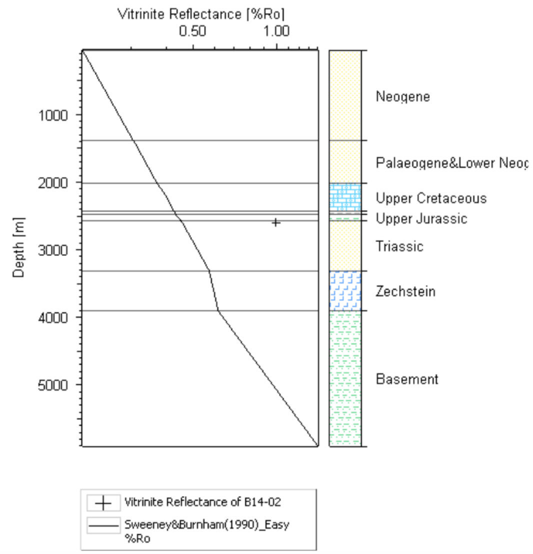


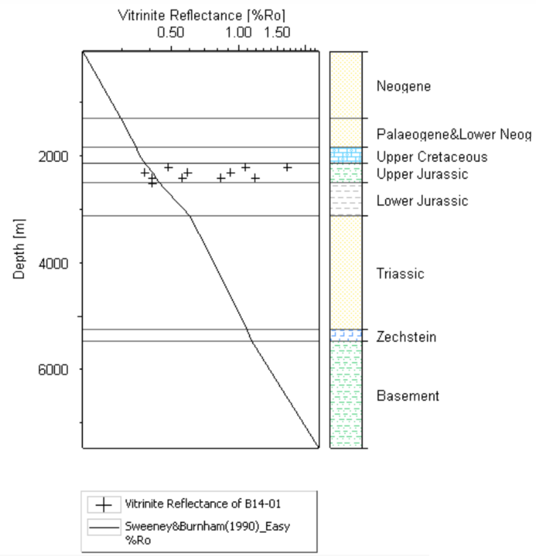


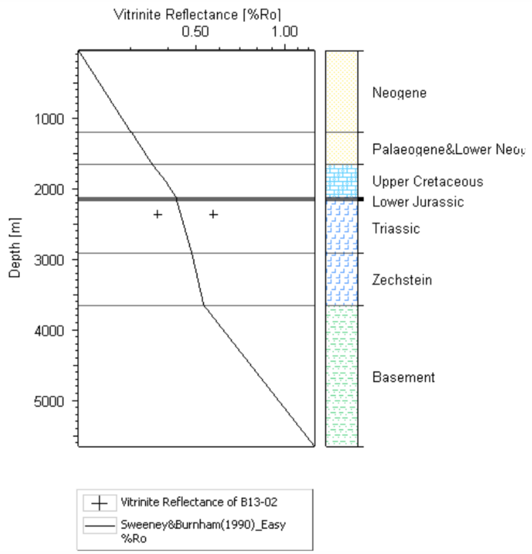


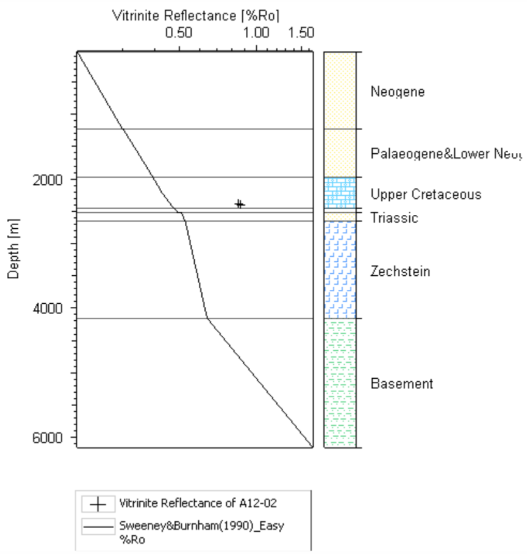


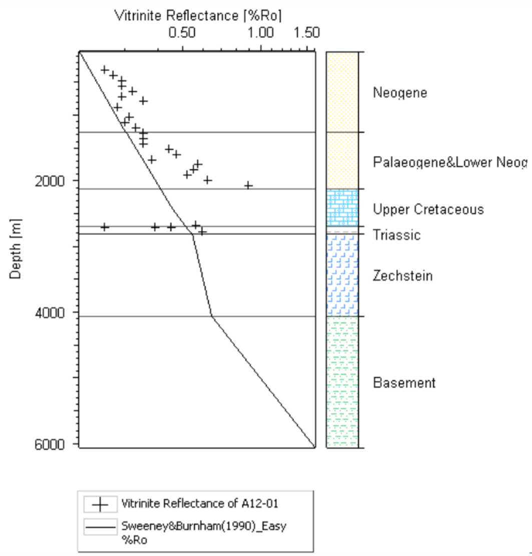


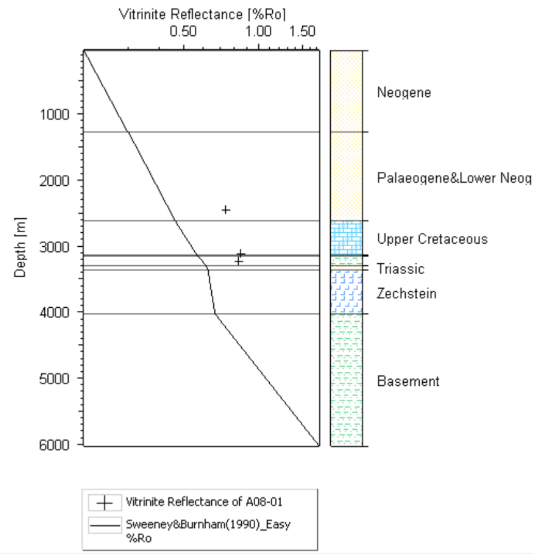

# Calibration alternative heat flow model